学校代码：10246
学　　号：18307110449

復旦大學

本 科 毕 业 论 文

G_2 规范理论在 $O5$ 平面上的五维膜网构造

5-brane webs with $O5$-plane for G_2 gauge theory

院　　系：　物理系
专　　业：　物理学
姓　　名：　陈艳艳
指 导 教 师：　Satoshi Nawata　青年研究员
完 成 日 期：　2022 年 8 月 6 日

指导小组成员

Satoshi Nawata　青年研究员

目　录

插图

摘　要

在弦论的第二次革命中，威滕证明了五种弦论——“I 型弦论”、“II A 型弦论”、” IIB 型弦论”、“$SO(32)$ 杂弦论”以及“$E_s \times E_s$ 杂弦论”共同起源于万有理论，他称之为“M 理论”。M 理论的基本要素不再是弦，而是膜（brane）。其中在 II 型弦论中，D 膜是被广泛研究的一大类，它的维度从 0 维到 9 维不等。在 IIA 型弦论中 D 膜空间维度必须是偶数维的，否则会破坏所有的超对称，而在 IIB 型弦论中 D 膜的空间维度是奇数维的。

D 膜被定义为高维空间中开弦端点驻足的子空间。在十维的闵氏时空里，开弦世界面作用量的运动方程告诉我们开弦的端点具有两种边界条件：一是诺伊曼边界条件，弦端点的法向导数为零，能够在该方向上以光速运动；二是狄利克雷边界条件，弦端点在该方向上处于静止状态，因此对应的坐标值是一个常数。当开弦的坐标 $x^0, x^1, \ldots, x^p$ 满足诺伊曼边界条件，$x^{p+1}, \ldots, x^9$ 满足狄利克雷边界条件时，我们会观察到运动的开弦端点仿佛是被约束在沿 $x^1, \ldots, x^p$ 方向伸展的超平面上。我们定义这个超平面为 Dp 膜，其中 p 代表 D 膜的维度。D 膜的存在破坏了时空原有的十维洛伦兹对称性，只有时间和作用诺伊曼边界条件的空间仍具有 $p+1$ 维的洛伦兹对称性。

D 膜在强耦合的超弦理论与 M 理论中作为一个强大的理论工具，引领了许多重大发现，例如黑洞热力学行为的微观物理、大 N 规范理论与引力的全息对偶等等。在弱耦合的弦论中，D 膜是一种带雷芒荷的非微扰物体，它可以终止在 NS（Neveu-Schwarz）膜上，形成网状结构用以描述规范理论，并帮助发现不同理论之间的对偶关系。膜网构造中一个简单的例子如两张平行的相同 D5 膜，能够用于描述五维的 SU(2) 规范理论。值得注意的是，在 D5 膜与 NS5 膜相交的地方，由于膜电荷守恒的量子效应，两张膜将会融合形成束缚态，即方向为 $(1,1)$ 的五维膜。更一般的，当 D5 膜（$(1,0)$ 膜）和 NS5 膜（$(0,1)$ 膜）的数量分别为互质的 p 和 q 时，最终形成的束缚态是 (p,q) 五维膜。

当我们需要描述例如正交群 $SO(N)$ 或辛群 $Sp(N)$ 的时候，我们需要进一步引入不可定向面（orientifold plane）的概念。“Orientifold” 是迹形（orbifold）和定向（orientation）的复合词。迹形的拓扑通常由奇异点（singularity）实现，远离这些点的空间是平坦的。五维不可定向面（O5-plane）平行于 D5 膜，它同时是一个 Z_2 迹形，具有 Z_2 反射对称性，会使一侧的 D5 膜镜像对称到另一侧。膜之间的开弦经过对称后，开弦的定向将会逆转。开弦并不会终止在 $O5$ 平面上，所以 $O5$ 平面并不是一个具有动力学的物体。相反，开弦可以终止在 D5 膜上，弦的激发能够引发 D5 膜的运动。$O5$ 平面由所带电荷不同分为四种类型，$\tilde{O}5^+$ 和 $O5^+$ 带 +1 的电荷，$O5^-$ 带-1 的电荷，$\tilde{O}5^-$ 带-1/2 的电荷。引入 $O5$ 平面后，我们能够构造 $Sp(2N)$ 和 $SO(2N)$ 规范理论对应的膜网结构。$Sp(2N)$ 是 N 个一致的 D5 膜堆叠在，$\tilde{O}5^+$ 平面上方，$SO(2N)$ 则是 N 个一致的 D5 膜堆叠在，$\tilde{O}5^-$ 平面上方。本论文主要研究的是 IIB 型弦论中 G_2 规范理论的五维膜网构造，及其对应的涅克拉索夫（Nekrasov）配分函数。第二章是对本文所需的 D 膜基础知识的简要概述，除前文所提的 D 膜定义，以及它与规范理论的联系外，还包括膜网形变的一些操作。

在第三章，我们展示了两种构造 G_2 规范理论五维膜网图的方法。一种是对纯规范理论 $SO(7)$ 并带一个旋量的五维膜网进行一次希格斯操作，另一种是基于 $SO(8)$ 的三隅对称性，对 $SO(8)$ 带一个旋量和一个共轭旋量的五维膜网进行两次希格斯操作。首先第一种构造方法需要先获得 $SO(7)$ 的五膜网图。$SO(2N-1)$ 的五膜网图可以从 $SO(2N)$ 和一个 flavor(在正交群 vector 表示下的超多重态) 的五膜网图中获得。其中 flavor 可以用 D7 膜来表示。一个 D7 膜与一个半无限长的单值分支（monodromy branch cut）相连。引入一个 D7 膜的目的是需要消去 $SO(8)$ 中包括镜像的八个 D5 膜中的一个 D5 膜。如果只关注 $O5$ 平面一侧的膜结构，我们就可以通过分离 D7 膜，然后将半个 D5 膜和半个单值分支与原有的 $O5^-$ 平面合并变成 $O5^-$-平面，最后得到 $SO(7)$ 的五膜网图。往 $SO(7)$ 中加入一个旋量，此时五膜网图中 $\tilde{O}5^+$ 平面、$(2,1)$ 五维膜、和 $SO(7)$ 中的 $(1,-1)$ 五维膜形成了一个局域的 E_2 结构。通过推广的 flop 变换，两个标准的 flop 变换以及希格斯（Higgsing）操作，我们得到了纯 G_2 规范理论的五维膜网图。需要指出的是，flop 变换前后五维膜网图具有物理不变性，而希格斯操作则不然。第二种构造方法是利用 $SO(8)$ 理论的三隅对称性，即

$$SO(8)+1V \iff SO(8)+1\bar{S} \iff SO(8)+1F。$$

因为第一种构造是对 $SO(7)$ 和一个旋量（spinor）进行一次希格斯操作，而 $SO(7)$ 又是由 $SO(8)$ 和一个在矢量表示（vector representation）下的 flavor 转变过来的。因此从 $SO(8)$ 和一个旋量 (S) 以及一个共轭旋量 $(\bar{S})$ 出发，经过两次希格斯操作，我们也应该会得到纯 G_2 规范理论的五维膜网图。如下图所示。我们只需仿照先前的流程，先对 $SO(8)+1\bar{S}+1S$ 的五维膜网图应用 flop 变换，但推广的 flop 变换根据 θ 角的不同对于旋量与共轭旋量有不同的变换形式。之后应用标准的 flop 变换和两次希格斯操作，我们就得到了 G_2 规范理论的另一种膜网构造。

另外，我们从有效初势（effective prepotential）的角度检验了两种构造方法的等价性。对有效初势的库伦分支模（Coulomb branch moduli）进行求导能够得到磁单极张力（monopole tension），它可以表达成膜网各区域面积的线性组合。我们发现两种构造都给出了一样的结论。经过希格斯操作而融合的几个区域都仅对同一个库伦分支模对应的磁单极张力有贡献。并且有一边与 $O5$ 平面重合的区域会有双重的贡献，这来源于 $O5$ 平面的反射对称性。此外，我们还利用计算初势和磁单极张力的方法，对纯 G_2 和纯 $SU(3)$ 且陈-西蒙斯数为 7 的理论之间的 S 对偶关系进行了初步的探究。其中 S 对偶是将 D5 膜和 NS5 膜的位置互换，也相当于将原来的五维膜网图进行 90° 逆时针的旋转，但所得的 $SU(3)$ 五膜网图中的 $O5$ 平面将变成 ON 平面。

在第四章，我们利用拓扑顶点形式计算了两种等价五膜网图的涅克拉索夫（Nekrasov）配分函数。拓扑顶点形式原本是是一种系统化的计算复曲面（toric）卡拉比-丘（Calabi-Yau）threefolds 的拓扑弦配分函数的方法。由于复曲面图和 IIB 型弦论中五膜网图的对应关系，这种方法也能够应用于五膜网配分函数的计算。它能够处理仅包含三价顶点的膜网图。我们对共用一个顶点的三条边标记不同的杨图，算出相应的顶点因子与边因子。最后的配分函数是所有顶点因子和边因子的乘积对所有杨图求和的形式。然而，传统的拓扑顶点形式并不能处理包含 $O5$ 平面的五膜网结构，但是我们可以利用 $O5$ 平面的性质，以及应用 flop 变换等来转换问题。

对于第一种 G_2 规范理论的膜网结构，我们应用了 O 顶点的方法。这个方法的主要思想

是将 $O5$ 平面和五维膜相交的顶点看作是一类新的顶点。我们可以通过引入标记空杨图的一条边，得到类似 E_2 结构的图，对该结构应用 flop 变换之后，再翻转一侧的膜得到带状的膜结构，此时就可以就应用传统的方法计算出 O 顶点对于的因子。O 顶点方法是传统拓扑顶点形式的有效推广。我们得到的最终的配分函数需要对三个杨图进行求和。

对于第二种 G_2 膜网构造，我们采用了剪切-粘贴的方法，主要做法是将最外层的五膜网关于 $O5$ 平面对称，然后沿中轴线剪开膜网，这样就得到了两组条带状的膜结构，此时可以应用传统的拓扑顶点形式去进行计算。最后我们还需要重新粘贴两组条带，这会引进一个新的结构因子。最终的配分函数需要对四个杨图进行求和。最后我们验证了两种结果呈现了非平凡的一致性。

关键字：五维膜网构造，G_2，有效初势，拓扑顶点形式，O 顶点
中图分类号：O413.1

Abstract

We display two kinds of 5-brane web constructions for pure G_2 gauge theories[3]. One is Higgsing the 5-webs of pure $SO(7)$ with one spinor, the other is Higgsing twice the 5-webs of $SO(8)$ with one spinor and one conjugate spinor, based on the triality of $SO(8)$ theories. In addition, we check the equivalence of two constructions,as well as the S-duality between pure G_2 and pure $SU(3)$ with Chern-Simons level 7, by effective prepotential. Finally, we manipulate the Nekrasov partition function of the two 5-brane web diagrams using topological vertex formalism, with which O-vertex method[4] and reflecting-gluing method are applied respectively. The results that we reproduce display a non-trivial identity.

Keywords: 5-brane web construction; G_2; effective prepotential; topological vertex formalism; O-vertex

CLC number: O413.1

第 1 章　Introduction

Before the Second String Revolution, a big problem that how the string theory provides description beyond perturbation theory has long attracted extensive attention. A significant breakthrough is the discovery of Dirichlet p-dimensional (Dp)-brane which serves as one of the non-perturbative objects in string theory. The Dp-brane can be seen as a spatial defect where an open fundamental string can end. It has a deep connection between gauge theories and thus acts as a powerful tool to understand the duality of different theories. Considering the Dp-branes end on the normal NS5-branes, we can draw a diagram that looks like a web, which still describes the same gauge theories. Furthermore, there is a quantum effect coming from the loop correlations in gauge theory that cause 5-branes to bend at the intersecting points. And the slope of the bent 5-brane is proportional to the net charge, which should obey the conversation law at intersecting points.

In type IIB string theories with eight supercharges, 5-brane web diagrams play an essential role in studying five-dimensional supersymmetric field theories. A 5-brane web diagram contains N coincidental D5-brane diagram can describe $SU(N)$ gauge theories. Nevertheless, to describe other gauge theories like $SO(N)$ and $Sp(2N)$, an orientifold plane needs to be introduced. An orientifold five-plane (O5-plane for short) can be regard as a five-dimensional space-time singularity parallel to the D5-brane. 'Orientifold' is a compound word of 'orientation' and 'orbifold', which imply its characteristic in some degree. More precisely, it is endowed with the abilities of reflecting branes above the plane to their mirror images, and also reversing the orientation of the strings which stretch between branes. Therefore the presence of the O5-plane instills a lot of fun into the brane engineering. To achieve the goal of constructing 5-brane diagrams of G_2 gauge theories, we have to utilize some deformation tools, like flop transitions[2] and Hanany-Witten transitions[5], to deform the 5-brane webs. These geometric transitions guarantee physical equivalence of the 5-brane web diagrams before and after the deformations[6].

The main focus of this article is to construct 5-brane web diagrams with $O5$-plane for pure G_2 gauge theories and to compute the corresponding Nekrasov partition functions, which have a far-reaching significance to studying the non-perturbative dynamics. In chapter 2, we give an introduction to the definition of Dp-branes and their dynamical properties. The 5-brane web constructions of the gauge theories $SU(N), SO(2N), Sp(2N)$ are also given, followed by a brief introduction of Higgsing process and Hanany-Witten transition.

In chapter 3, we give two ways of construction the 5-brane web diagrams for pure G_2 gauge theories. The starting point of the first approach is the 5-webs of pure $SO(7)$. When constructing 5-brane web diagrams for $SO(7)$, a D7-brane with a monodromy branch cut is involved to solve the fractional charge difference problem on O5-plane. Higgsing the 5-brane web diagram of $SO(7)$ with one spinor will yield a diagram for pure G_2. The other approach is based on the triality of $SO(8)$

theories. We start form 5-brane web diagram $SO(8)$ with one spinor and one conjugate spinor, and Higgs it twice. Eventually, we derive the desirable diagram of pure G_2. These two constructions and also the S-duality between G_2 and pure $SU(3)$ with Chern-Simons level $\kappa = 7$ are checked from effective prepotential later.

In chapter 4, the Nekrasov partition functions of the two 5-brane web diagrams with O5-plane for G_2 are computed by the topological vertex formalism, but using different ways. We apply the O-vertex method to the first 5-brane construction for G_2. The O-vertex is a vertex where a 5-brane intersects with O5-plane and we obtain its formulation by a simple example. Then the partition function is a sum over the product of all vertex factors and edge factors, together with the factors from the O-vertex. Since the second 5-brane web diagram is bilateral symmetry, and there is a more skillful approach to manipulate the partition function. First the reflection of the out-most 5-branes with respect to the O5-plane will give a diagram similar to $SU(4)$. And then we cut it into halves, the partition function of the strip diagrams can be straightforward computed. The subsequent gluing process will generate an extra factor. We make a comparison of their instanton partition functions and find that they produce the same results.

第 2 章　Fundamentals

2.1　Introduction to the 5-branes

In this section, we will briefly review the five-dimensional setup in type IIB string theory, and discuss the brane constructions of gauge groups $SO(N)$ and $Sp(N)$[7, 8].

2.1.1　Dp-brane

The brane configurations live in ten-dimensional Minkowski spacetime with the time coordinate x^0 and space coordinates $x^1, x^2, \ldots, x^9$. A Dirichlet p-dimensional brane (Dp-brane) comes from imposing the boundary conditions on open strings. There are two kinds of boundary conditions which arise from the variation principle of the open string action:

$$\begin{aligned} \text{Neumann boundary condition: } \partial_\sigma X^\mu = 0 \quad \text{at } \sigma = 0, \pi; \\ \text{Dirichlet boundary condition: } \delta X = 0 \quad \text{at } \sigma = 0, \pi, \end{aligned} \tag{2.1}$$

where σ means the world-sheet spatial coordinate of the open string and X denotes its space-time coordinate.

Now we can see that the Dirichlet boundary condition has stronger constraints on the endpoints of the open strings since X should be constant. Consider a bunch of open strings whose coordinate components $x^0, x^1, \ldots, x^p$ satisfy the Neumann boundary condition and $x^{p+1}, \ldots, x^9$ satisfy Dirichlet boundary condition. Then it seems that the open strings are constrained on a Dp-brane which stretches in $(x^1, \ldots, x^p)$ hyperplane and locates at $(x^{p+1}, \ldots, x^9)$. For type IIB string theory, p is always odd($p = -1, 1, 3, 5, 7, 9$). Particularly, $p = 1$ brane is the D-instanton, while $p = 9$ is a $(9+1)$-dimensional object filling the whole space-time. Moreover, D9-branes can turn the type IIB string theory into type I string theory with orientifolds. We can regard the Dp-branes as the spacetime defects where the fundamental strings can end. Then the presence of the Dp-branes breaks the translation and Lorentz symmetries of the Minkowski spacetime to a subspace of *Poincare* $(1, p) \times SO(9-p)$, where $SO(9-p)$ is the rotation symmetry of the Dp-brane around its normal axis $x^{p+1}, \ldots, x^9$. Furthermore, the excitations of the open strings which end on Dp-branes can endow the Dp-branes with dynamics. So by quantizing these open strings, we will get a massless vector field A_μ and $9-p$ massless scalar fields Φ^a ($\mu = 0, 1, \ldots, p$ and $a = p+1, \ldots, 9$). Note that the number of scalar fields is equal to the number of transverse directions of a Dp-brane and thus they can describe fluctuations of the Dp-brane in transverse directions.

2.1.2　N_c coincidental Dp-branes

At the moment, let us consider the configuration composed of N_c color Dp-branes. The schematic diagram 2-1 is borrowed from the reference[1]. Figure (a) shows a fundamental string with both ends

on a single Dp-brane, and there is $U(1)$ global symmetry for the string interactions. Generalize it to the case of a stack of N_c distinguishable Dp-branes, the global symmetry for string interactions become $U(1) \times U(1) \times \ldots \times U(1)$ (N_c times) now which is the gauge symmetry in the spacetime of the worldvolume of Dp-branes as well. Note that only the open strings with both endpoints on the same Dp-branes can yield massless states. Otherwise, they will give massive states due to the tension of strings.

Now assume that these N_c Dp-branes are coincidental, then the gauge symmetry will get enhanced to be $U(N)$. Figure (b) shows that there will be a $U(N_c)$ gauge field $(A_\mu)_{ij}$ and $9-p$ scalars $(\Phi^a)_{ij}$. The scalar field $(\Phi^a)_{ij}$ becomes a $N_c \times N_c$ matrix transforming under the adjoint representation of the $U(N_c)$ group. The (i, j) element of A_μ and Φ^a corresponds to the fundamental string with one end on the i-th Dp-brane and the other end on the j-th Dp-brane. Also note that the open string with its endpoints on whichever Dp-branes will yield massless states, for the reason that any open string stretched between two Dp-branes can achieve vanishing length. And it implies that the coincidental Dp-branes will exert no force to each other.

Since those paralleled Dp-branes are indistinguishable from each other, they will stay the same after any kind of rearrangements, which implies that the configuration are endowed with the cyclic symmetry S_n. Moreover, the position of each Dp-brane is represented by a $9-p$-vector $(x^{p+1}, \ldots, x^9)$ and thus the total degree of freedom is $(9-p)N_c$. Thus the moduli space is $(\mathbb{R}^{9-p})^{N_c}/S_{N_c}$.

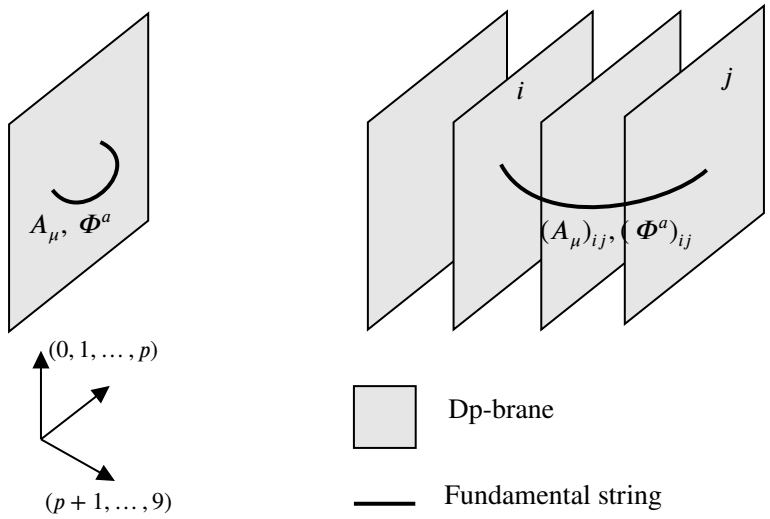

图 2-1 Fundamental strings with both ends on Dp-branes depict (a) a $U(1)$ gauge field and $9-p$ scalars on a single Dp-brane, or (b) a $U(N_c)$ gauge field and $9-p$ scalars on a stack of N_c coincidental Dp-branes[1]

2.1.3 (p, q) 5-brane

To discuss about the 5-brane web construction for various gauge theories, I use the notation in the reference[7] for the worldvolumes of different branes as shown in the table below. Note that the p NS 5-branes and q D5-branes are perpendicular in the $x^5 - x^6$ plane, so they will intersect with each other, and finally merge into a bound state called a (p, q) 5-brane (fig:2-2). Here (p, q) should be a co-prime pair[9]. Otherwise, we can view the (p, q) 5-branes as a collection of m_0 (p_0, q_0) 5-branes when $(p, q) = m_0(p_0, q_0)$ with p_0 and q_0 relatively prime. Those (p, q) 5-branes behave like

	x^0	x^1	x^2	x^3	x^4	x^5	x^6	x^7	x^8	x^9
NS5	x	x	x	x	x	x	o	o	o	o
D5	x	x	x	x	x	o	x	o	o	o
D7	x	x	x	x	x	o	o	x	x	x

表 2-1 The worldvolumes of different branes

standard 5-branes but with residual $SL(2,\mathbb{Z})$ symmetry. Also, the presence of the (p,q) 5-branes break the spacetime Lorentz symmetry from $SO(1,9)$ to $SO(1,4)\times SO(3)$, where $SO(1,4)$ is the Lorentz symmetry of the five-dimensional spacetime and the double cover of $SO(3)$ is exactly the five-dimensional R-symmetry. In this notation, D5-branes can be viewed as (1,0) 5-branes while NS 5-branes can be viewed as (0,1) 5-branes. The conversation of charge at vertex requires

$$\sum_i p_i = 0, \quad \sum_i q_i = 0, \tag{2.2}$$

so the afore-mentioned emerging process satisfies the conversation law naturally.

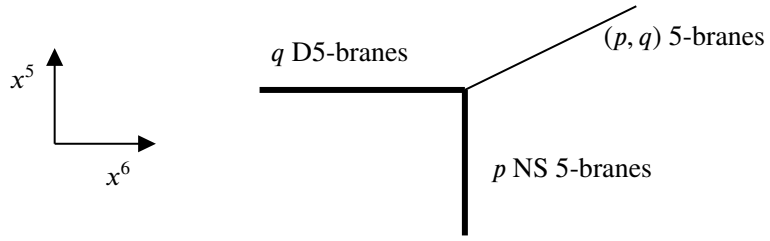

图 2-2 p D5-branes and q NS 5-branes merge into (p,q) 5-branes, which implements conservation of charge at the vertex

2.2 5-brane web configurations for gauge groups

The boundary conditions can tell which gauge groups the brane configurations describe. To pave the way for constructing G_2 gauge theories, we are going to talk about the brane configurations for the gauge groups $SU(N)$, $SO(N)$ and $Sp(N)$.

2.2.1 Brane webs for gauge group $SU(N)$

As mentioned in subsection 2.1.2, the N_c coincidental D5-brane will give rise to a $U(N_c)$ gauge group. Figure 2-3 (a) shows the web configuration of pure $SU(2)$ gauge theory more succinctly, and all the parallel D5-branes are coincidental although they are drawn separately. Since D5-branes must end on NS5-branes, and the fundamental open strings should end on the D5-brane as before, the gauge group arising from the boundary conditions of the strings will stay the same. Generally speaking, let us denote the number of the horizontal color D5-branes by N_c, then the overlapping N_c D5-branes stretched between the vertical NS5-branes depict the pure $SU(N_c)$ gauge theory. In the quantum level, we should take the charges into account, then the NS5-branes will bend at the vertex according to the conservation law (2.2). Figure (b) stands for the case of adding quark flavors

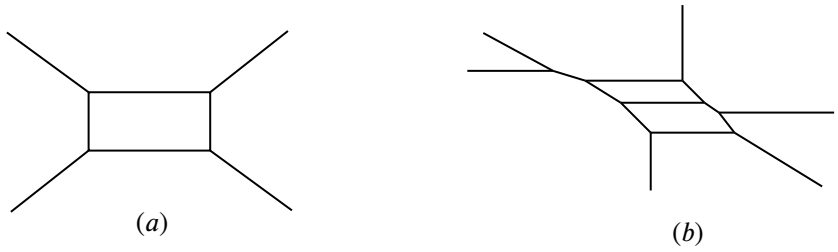

图 2-3 (a) pure $SU(2)$, (b) $N_f = 2, N_c = 3$ SQCD

(hypermultiplets in the fundamental representation) to the pure $SU(N_c)$ theory. The quark flavors are represented by the semi-infinite horizontal branes, and their number is denoted by N_f, resulting here in a $N_f = 2, N_c = 3$ SQCD theory.

2.2.2 Orientifold 5-planes

To derive the web configuration of the orthogonal groups and the sympletic groups, it is vital to introduce an orientifold 5-plane ($O5$-plane for short) which is parallel to the D5-brane. The 'orientifold' got its name from 'orientation reversal' and 'orbifold'. The reasons are that it can be thought as a $\mathbb{Z}_2$ orbifold fixed plane due to the $\mathbb{Z}_2$-symmetry acting on the spacetime coordinates, and additionally, it can reverse the orientation of the strings after the reflection. The role of an $O5$-plane is to serve as a mirror to reflect the D5-branes on the one side to the other side, and the strings can stretch between D5-branes and their mirror images. Unlike the D5-branes, there are no string modes that are tied to the $O5$-planes to generate the fluctuations, so they are non-dynamical.

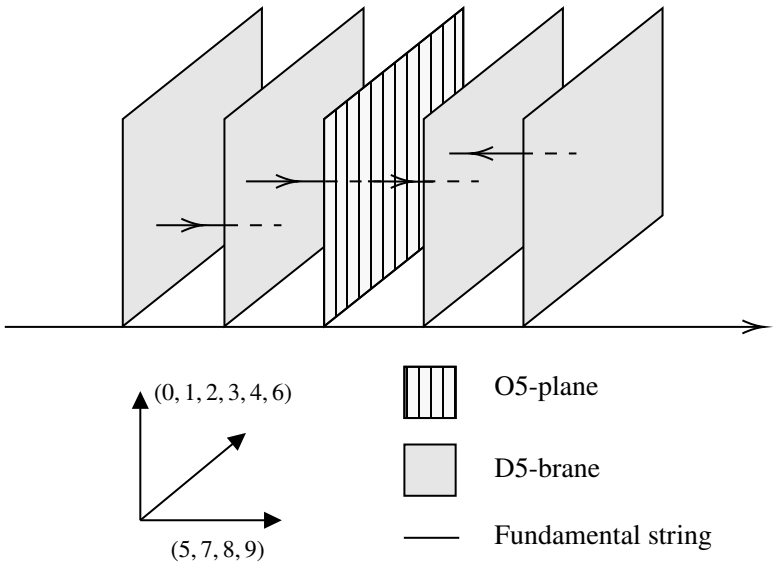

图 2-4 An $O5$-plane with two adjacent D5-branes and their mirror images. The fundamental string stretching between a D5-brane and its mirror image will reverse its orientation after reflecting with respect to the $O5$-plane.

There are four kinds of $O5$-planes denoted as $O5^+$, $O5^-$, $\tilde{O}5^+$ and $\tilde{O}5^-$. The main difference between them is the amount of D5-brane charge that they carry. The $O5^+$ and $\tilde{O}5^+$ carry charge $+1$, while the $O5^-$ carries charge -1 and the $\tilde{O}5^-$ carries charge $-\frac{1}{2}$.[10] At the moment, one can imagine the case that a half NS5-brane crosses an $O5$-plane, and its classical picture is demonstrated as figure

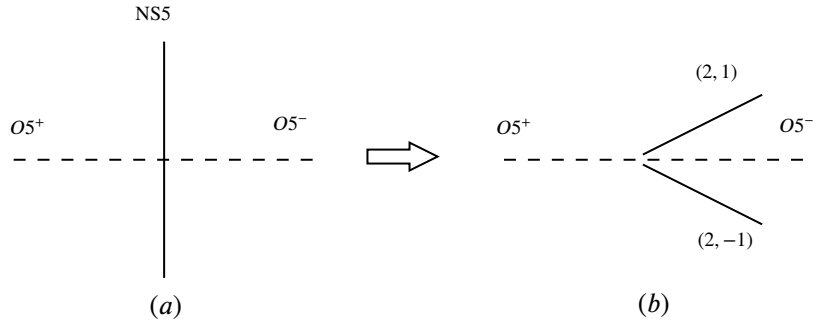

图 2-5 (a) The classical picture of a NS5-brane intersecting with an $O5$-plane. The NS5-brane is represented as a solid vertical line and the $O5$-plane is displayed by a horizontal dashed line. (b) In the quantum picture, the conversation of charges carried by D5-brane requires the NS5-brane to bend.

2-5 (a). To preserve $\mathcal{N} = 1$ supersymmetry, the NS5-brane crossing the $O5$-plane will partition the $O5$-plane into two parts of different signs and charges. In other words, the $O5$-plane will change its type form $O5^+(\tilde{O}5^+)$ to $O5^-(\tilde{O}5^-)$ when it passes through the NS5-brane. When it comes to the quantum level, we will find there exists a jump of D5-brane charge at the intersecting point. Thus the conversation law of charges requires the NS5-brane to bend as it is shown in 2-5 (b).

2.2.3 Brane webs with an $O5$-plane for gauge groups $SO(N)$ and $Sp(N)$

There are several ways to construct web diagrams for the gauge groups $SO(N)$ and $Sp(N)$. And here we will briefly introduce the web configurations in the presence of an $O5$-plane which describe $SO(N)$ and $Sp(N)$.

Firstly, the web configuration of $Sp(N)$ ($N = 2N_c$) with N even is displayed by figure 2-6 (a). It is produced by putting N D5-branes on the top of an $O5^+$-plane or an $\tilde{O}5^+$-plane. The thick lines means that there is a stack of D5-branes, while the thin line means the NS5-brane. The charge conservation equations 2.2 accounts for the slope of the bent NS5 branes.

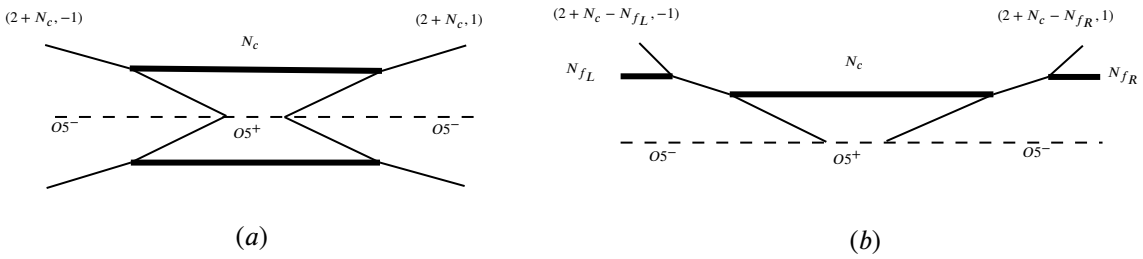

图 2-6 (a) $Sp(2N_c)$ (b) $Sp(2N_c)$ with $(N_{f_L} + N_{f_R})$ flavors

If one wants to add some flavors, the semi-infinite horizontal D5-branes, which end on NS5-branes as well, should be added to figure (a) to derive figure (b). Then an open string connect a left (right) semi-infinite D5-brane and the left (right) NS5-brane will yield a massless flavor hypermultiplet. However, this method of adding flavors will affect the asymptotic space-time geometry. As we can see when $N_{f_L} + N_{f_R} = 2N_c + 4$, the two NS5-branes become parallel to each other. And when $N_{f_L} + N_{f_R} > 2N_c + 4$, the two NS5-branes may have an intersection in the distance. Alternatively,

We have another way to add flavors by making use of D7-branes. The worldvolume of a D7-brane is given in the table 2-1, so a D7-brane is like a point in the $x^5 - x^6$ plane. A D7-brane is connected with the 5-brane webs for pure gauge theories by a horizontal D5-brane. Then the addition of flavors can be done by pulling out all the D7-branes in the same direction and it will result in semi-infinite D5-branes. The advantage of introducing the D7-brane will be further illustrated in the latter section 3.1.

Similarly, the web configuration for $SO(2N)$ is constructed by putting $N(N = N_c)$ D5-branes on the top of an $O5^-$-plane, as shown in figure 2-7. The ways of adding flavors are always the same as the case of $Sp(2N)$. To guarantee that the external NS5-branes do not intersect with each other, N_c should be larger than one, and also $N_{f_L} + N_{f_R} <= 2N - 4$. As for $SO(2N + 1)$, we should replace the $O5^-$-plane by $\tilde{O}5^-$-plane at first. Then 5-brane web diagrams for $SO(2N + 1)$ can be derived from the Higgsing the 5-brane web diagrams of $SO(2N+2)+1F$ ($1F$ stands for one flavor), in the presence of $\tilde{O}5^-$-planes[10]. More details will also be further discussed in the latter section 3.1.

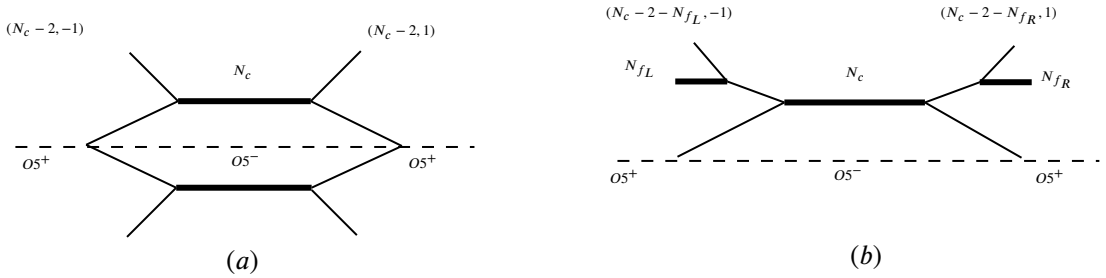

图 2-7 (a) $SO(2N_c)$, (b) $SO(2N_c)$ with $(N_{f_L} + N_{f_R})$ flavors

2.3 Deformations of 5-brane web diagrams

2.3.1 The Higgs branch

All the continuous deformations of the web diagrams form the moduli space in 5d gauge theory, among which the deformations in and off the plane of the Webs correspond to the coulomb branch and the Higgs branch respectively. The Higgs branch can be entered upon separating the sub-Webs from the original web configuration. Note that a web configuration is reducible if it consists of two or more independent sub-Webs. And the process of reducing the Webs is exactly a process of finding roots for the Higgs branch. During Higgsing, the rank of the local gauge group will be decreased by one, and the 5d R-symmetry $SO(3) = Sp(1)_R$ will be broken.

Generally, the Higgs branch contains two ways to perform: one is giving a VEV to a meson, and the other is giving a VEV to a baryon.

As a simple example, let us consider the 5-brane web diagram of $SU(N_c)$ theory with $N_c = 3$ and $N_f = 4$. As it is shown in figure 2-8 (a) below, there are three horizontal color branes and four semi-infinite flavor branes. Additionally, the distinction between the left and right semi-infinite branes, which are associated with two kinds of hypermultiplets respectively, lies in the sign difference of their masses. In 5d theory, the masses of multiplets are always real, and therefore

we can distinguish the left and the right semi-infinite branes by equipping them with positive and negative masses, or vice versa.

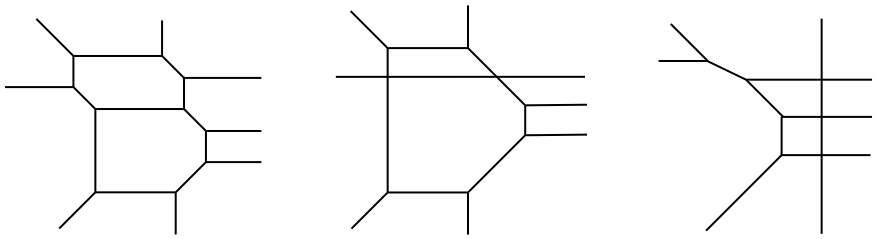

图 2-8 (a) 5-brane diagram for $SU(N_c)$ theory with $N_c = 3$ and $N_f = 4$. (b) a root for a mesonic branch, (c) a root for a baryonic branch

First, to construct a gauge-invariant meson, we need two semi-infinite branes on both the left and right sides, and each corresponds to a quark flavor. As shown in figure 2-8 (b), by moving up the horizontal color brane in the middle and making it align with the two semi-infinite flavor branes, we can separate these three branes as a sub-Web from the original Webs. This Higgsing process of reducing 5-brane web diagrams enables us to find a root for a mesonic branch. Also, we can see that the rank of the local gauge group is decreased by one since the number of faces in the 5-brane web diagram is decreased by one.

Second, giving a VEV to a baryon requires us to align the N_c(i.e.3 in our example) color branes with the same number of the semi-infinite branes, as shown in figure 2-8 (c). As a result, we separate the vertical lines as a sub-Web from the original diagram (a). In fact, this deformation is related to a Fayet-Iliopoulos term, and therefore it explain why the process is called giving a VEV to a baryon.

Moreover, we can also determine the number of sub-Webs in the given 5-brane web diagram. List all the 2d vectors $(p, q)_i$ for the external legs and it's easy to see the sum of all these 2d vectors is zero. Note that each sub-Web that can be separated from the original Web must sum to zero. So the total number of sub-Webs is exactly the number of subsets satisfying zero-sum in the list.

$$\#(\text{sub-Webs}) = \#(\text{zero-sum subsets of the } (p, q) \text{ lists for external legs}) \tag{2.3}$$

2.3.2 The Hanany-Witten transition

In this subsection, we will partly follow the logic of the Hanany and Witten's work[5], in which new brane dynamics were discovered that a third brane can be created or annihilated when two branes cross. For the sake of convenience, we stick to their notation of worldvolumes below.

	x^0	x^1	x^2	x^3	x^4	x^5	x^6	x^7	x^8	x^9
NS5	x	x	x	x	x	x	o	o	o	o
D5	x	x	x	o	o	o	o	x	x	x
D3	x	x	x	o	o	o	x	o	o	o

表 2-2 The worldvolumes of different branes

The mechanism can be illustrated by a simple example shown in figure 2-9. It contains a D3-brane, a D5-brane and two NS5-branes. Since the latter two kinds of branes have two more spatial dimensions than a D3-brane, they are thought to be much heavier. Technically we can regard the position parameters of D5-branes and NS5-branes to be fixed, which are denoted by $(t, \vec{w}), (z, \vec{m})$ respectively. Note that z and t both parameterize x^6 direction, while $\vec{w}$ is a vector in (x^7, x^8, x^9), together with $\vec{m}$ as a vector in (x^3, x^4, x^5). These parameters can also be interpreted as a coupling constants on the D3-brane worldvolume.

As shown in (a), the horizontal D3-brane stretches in the x^6 direction, whose transverse position in x^3, x^4, x^5 directions is $\vec{x}$ and in x^6, x^7, x^8 directions is $\vec{y}$. According to the table 2-2, the two NS5-branes and the D5-brane are perpendicular to it with position parameters $(t_1, \vec{w}_1), (t_2, \vec{w}_2), (z, \vec{m})$ respectively. As an initial state, we have $t_1 < z < t_2$ in (a), and the hypermultiplet raising from a string between the D3-brane and D5-brane has mass proportional to $|\vec{m}-\vec{x}|$. Especially when $\vec{m} = \vec{x}$, the D3-brane and the D5-brane actually meet in space, so an elementary superstring connecting them will give rise to a massless magnetic hypermultiplet.

As we increase z, the D5-brane will cross the NS5-brane eventually. We may expect the configure to be like figure (b), where $t_1 < t_2 < z$. Nevertheless, a paradox appears in this case because there no longer exists a mechanism to derive a massless hypermultiplet even under the situation $\vec{m} = \vec{x}$. Also, there's no reason for the hypermultiplet to decay in this case.

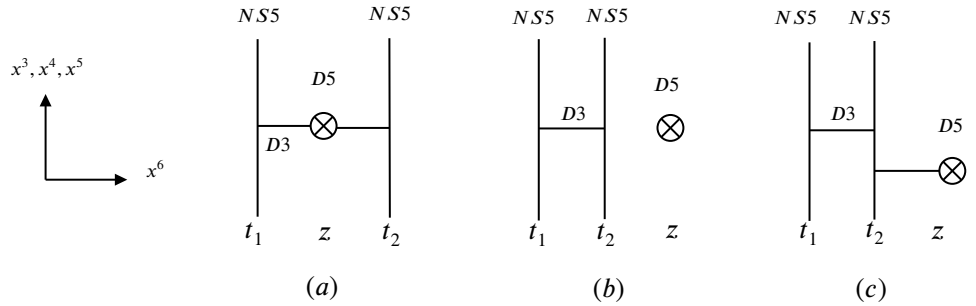

图 2-9 The process of a D5-brane crossing a NS5-brane. (a) The initial configuration. (b) The naive configuration of moving D5-brane to the right. It will cause a paradox. (c) The corrected configuration by adding an extra D3-brane.

So the problem can be fixed if we consider an extra D3-brane is created which connects the D5-brane and right NS5-brane after the crossing happens. It is depicted in figure (c). Note that one end of the D3-brane touching the D5-brane indicates $\vec{x} = \vec{m}$, and the other end requires $\vec{y} = \vec{w}_2$. Consequently, the D3-brane with all position parameters fixed will contribute no moduli to the configuration. In other words, all the three configurations are endowed with the same moduli. In contrast to figure (b), figure (c) can have a mechanism to get a massless hypermultiplet. We can tune the position parameters $\vec{x}$ of both D3-branes to be equal, then the elementary string connecting the two aligned D3-branes will associate to a massless hypermultiplet.

Conversely, when we move the D5-brane in figure (c) crossing the NS5-brane to the left, we should derive figure (a), and a D3-brane will be annihilated accordingly.

This proposal of creating or annihilating a D3-brane was deemed essential using a propri argument on the consequent phenomenon, such as the invariant linking number in the compact cases and

the conserved total magnetic charge in the noncompact situation. But we will not explain in detail in this article.

More generally in Type IIB theory, a Dp-brane can be created or annihilated when a D(p+2)-brane crosses a NS5-brane. We will make use of this conclusion in the construction of 5-brane web diagram for G_2 theories, which involves a D7-brane as a flavor.

第 3 章　Two Constructions of 5-Brane Webs for G_2 Gauge Theories

3.1　From $SO(7)$ gauge theory with one spinor

In this section, we will construct a 5-brane web diagram in the presence of $\tilde{O}5$-plane for G_2 gauge theory. The starting point is that the 5-brane diagram of $SO(7)$ with one spinor can be transformed to a 5-brane web diagram of pure G_2 by a Higgsing procedure[3]. However, when we get started to construct a 5-brane web diagram with $\tilde{O}5$-plane for pure $SO(7)$, we will encounter a barrier immediately. Note that the NS5-brane partitions the $\tilde{O}5$-plane into two parts $\tilde{O}5^+$ and $\tilde{O}5^-$. And the difference of charges between two types of orientifold 5-planes is fractional. It appears to be impossible to reconcile the bending of the NS5-brane to satisfy the charge conservation law because the slope (p, q) should be represented as a co-prime pair. A way out is to decompose an $\tilde{O}5^-$-plane into an $O5^-$-plane and a half D5-brane, together with a half monodromy arising from the a half D7-brane, in the sense that we only focus on the upper half diagram. Then the initial fractional difference of charge can be changed to an integer.

3.1.1　5-brane web diagram for pure $SO(7)$

We have discussed a general way to construct the 5-brane webs with $O5$-plane for $SO(2N)$ and add flavors by D7-branes in subsection 2.2.3. So here we will construct the 5-brane web diagrams using $\tilde{O}5$-plane for $SO(7)$, starting from the web diagrams of $SO(8) + 1F$ using $O5$-plane, and the method is applicable to the case of pure $SO(2N + 1)$ for any N. To begin with, we add one flavor to the $SO(8)$ diagram by D7-branes, as shown in figure 3-1 (a).

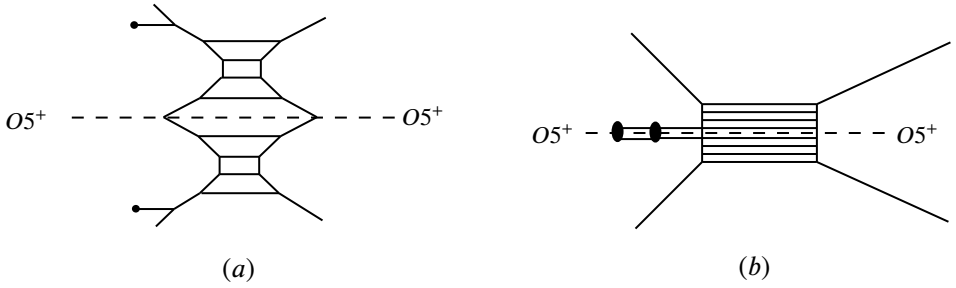

图 3-1　(a) The web for $SO(8) + 1F$. (b) The web at the origin of the Coulomb branch and massless flavor, after separating the D7-brane and its image.

To enter the Higgs branch, we can go to the origin of the Coulomb branch (figure 3-1 (b)). By coalescing all the D5-branes on the $O5$-plane, we can reach the limit of zero mass of flavors since the strings connecting the semi-infinite D5-branes and other finite D5-branes can have vanishing

length. Note that once an $O5^+$-plane passes through a D7-brane, it transforms to an $\tilde{O}5^+$-plane. So after separating the D7-brane from its image on the $O5^+$-plane, there is an $\tilde{O}5^+$-plane between two D7-branes. However, a D5-brane which stretches between the D7-branes cannot be stuck on an $\tilde{O}5^+$-plane, so it forces us to put an extra D5-brane between the D7-branes. Moreover, the process of separating D7-branes and adding an extra D5-brane can be thought as moving the separating D7-branes past the bent NS5-brane(more precisely we will use $(2,1)$ 5-brane later) on $O5$-plane. The slope of $(2,1)$ 5-brane will change to $(3,1)$ according to charge conversation. Figure 3-2 illustrates this process in more detail.

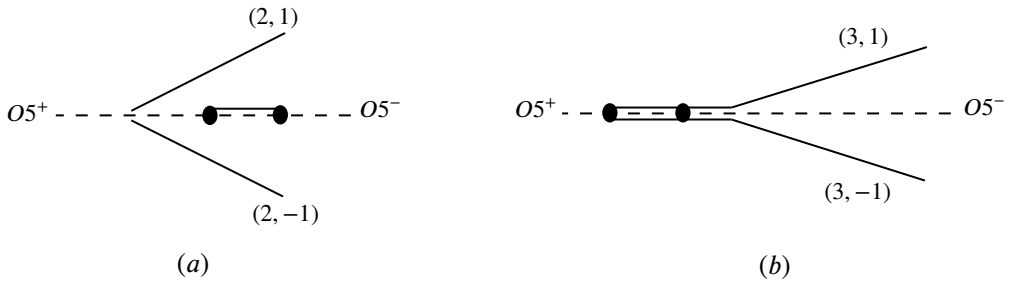

图 3-2　(a) Separating D7-brane and its image. (b) Moving them past the bent NS5-brane.

From figure 3-1 (a), we move the D7-branes and also the D5-branes nearest to the $O5$-plane, along the left bent NS5-brane to the $O5$-plane. And separating the D7-brane from its image with an additional D5-brane ending on them, we derive the first diagram in figure 3-3. In fact, there exists some subtlety between the whole diagram and the upper half diagram with the $O5$-plane. When we consider the whole diagram, including the mirror image, the charge of $O5$-plane should be doubled in the charge conversation equation. In this sense, we can regard that a D5-brane stuck on the $O5$-plane is divided and remains a half for the upper half plane. The black dot on the $O5$-plane stands for a full D7-brane. Since D7-brane can change the types of $O5$-plane as mentioned before, we can regard that there is a monodromy associated to a D7-brane. Here we denote the two monodromy lines of the two D7-branes by a dotted line stretching in the left direction in (a). Figure (b) is the web for $SO(7)$ after one enters the Higgs branch of (a). We move the left D7-brane to infinitely right and remove the two D5-branes stretching between them, so the original $O5^+$-plane can be coalesced with the monodromy to get an $\tilde{O}5^+$-plane.

By pulling out the other D7-brane to the right side, we notice that a monodromy stuck on the $O5^-$-plane will yield a $\tilde{O}5^-$-plane between the $(2,1)$ 5-brane and the $(1,-1)$ 5-brane (figure (c)). Here the D5-brane connecting the D7-brane is annihilated due to the Hanany-Witten transition. Taking the D5-brane into account, again we see the reason why introducing the D7-brane and its monodromy can fix the fractional charge problem at the beginning of this section. Note that the stuck D5-brane on $\tilde{O}5^-$-plane becomes a half D5-brane if we ignore the lower half diagram, so the statement here is consistent with that in the beginning of this chapter. Finally, we plug the D7-brane to infinitely left, we get figure (d), which is the 5-brane web diagram for pure $SO(7)$ gauge theory.

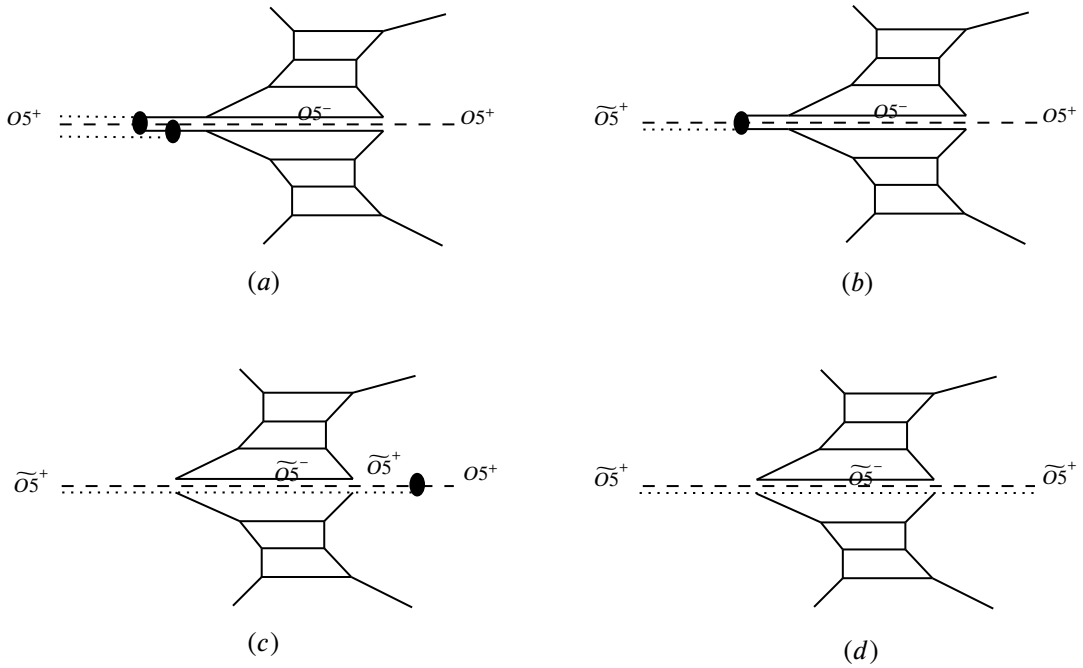

图 3-3 (a) Equivalent diagram to $SO(8)+1F$ in figure 3-1, after moving and separating D7-branes on $O5$-plane. The monodromy branch cut is denoted by a black dotted line, which is associated to a D7-brane. The D5-brane stuck to the $O5$-plane is denoted by a black solid line. The $O5$-plane of any kind is denoted by a black dash line. (b) The web diagram for $SO(7)$ arising from entering the Higgs branch of $SO(8)+1F$. (c) Pull out the D7-brane to the right side. The $O5$ will transform into $\tilde{O}5$ when the D7-brane passes through it. One can check the charge conversation law at the two intersecting points. (d) Move the D7-brane to infinitely right. The resulting diagram is the whole 5-brane web diagram for pure $SO7$ gauge theories.

3.1.2 5-brane web diagram for pure G_2

Initially, it is straightforward to add a spinor (a hypermultiplet in the spinor representation) to the 5-brane web diagram of the pure $SO(7)$ gauge theory. For convenience, let us ignore the lower half plane from now on. Figure 3-4 demonstrates a 5-brane web diagram for the $[1]-SO(9)-Sp(2)-[\frac{3}{2}]$ quiver theory[3]. Here $[n]-G$ means that there are n flavors attached to the G gauge theory. In figure 3-4 (a), we draw the half D5-branes by red solid lines, then we can see there are $\frac{5}{2}$ semi-infinite D5-branes in total, with the half semi-infinite D5-brane thereof stuck on the $\tilde{O}5^-$-plane. A Higgs branch becomes manifest in this theory as we align the two semi-infinite D5-branes with the two finite D5-branes on the top of $\tilde{O}5^-$-plane and $\tilde{O}5^+$-plane. As a result, it yields figure 3-4 (b) after moving off the infinite D5-brane. Before Higgsing, the $SO(9)$ gauge theory is coupled with the $Sp(2)$ gauge group. And the inverse of gauge coupling is related to the mass of the $Sp(2)$ instantons, which carry charge in the spinor representation of $SO(9)$. While after Higgsing, diagram (b) looks similar to that of the pure $SO(7)$ gauge theory, but the gauge coupling of the "$Sp(0)$" gauge group still remains. Then we can imagine that the inverse of the gauge coupling may correspond to the mass of the "$Sp(0)$" instantons. Thus we can regard figure (b) as an $SO(7)$ gauge theory with a spinor[3].

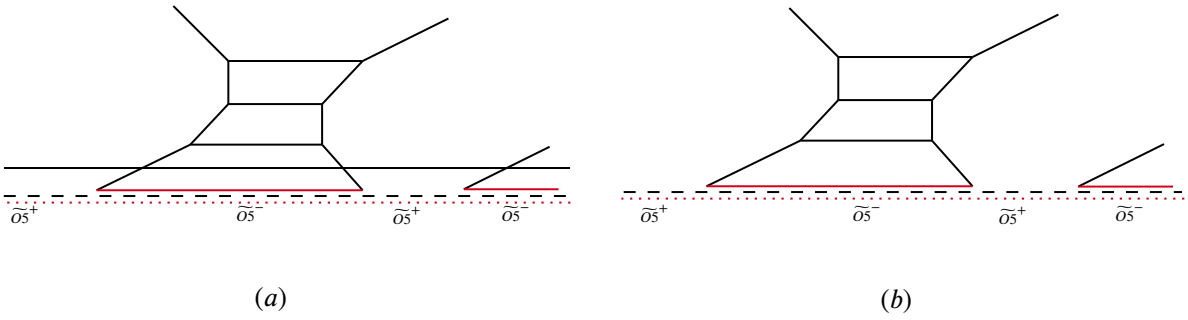

(a) (b)

图 3-4 (a) A 5-brane web diagram for $[1]-SO(9)-Sp(2)-[\frac{3}{2}]$. The red solid line stands for a half D5-brane and the red dotted line denotes a half monodromy. (b) $SO(7)$ with one spinor matter derived by Higgsing figure (a).

We observed that there exists a $SU(2)$ gauge symmetry for the flavors given by the string stretching between the two external $(2,1)$ 5-branes. And it also serves as a global symmetry acting on the spinor. Then the mass of the spinor is related to the distance between these two parallel $(2,1)$ 5-branes. To enter the Higgs branch, we try to take the zero mass limit. However, we will meet a thorny dilemma to transform the diagram with $\tilde{O}5$-plane by conventional "flop" transition. Fortunately, we can also turn to another equivalent diagram for $SO(7)$ with one spinor, which is depicted in figure 3-5. It is obtained from figure 3-3 (b) by directly pulling out the D7-brane to the infinitely left and adding a spinor, which is from the coupling of pure $SO(7)$ and $Sp(0)$. Now figure has a full semi-infinite D5-brane stuck on the $O5$-plane. We find that the $(1,-1)$ 5-brane and the $(2,1)$ 5-brane, together with the $O5^+$-plane in between, form a local diagram for E_2 gauge theory. Thus we can apply a generalized flop transition to it, ignoring the surroundings of this local structure.

The generalized flop transition of the local E_2 brane diagram yields two possible consequences

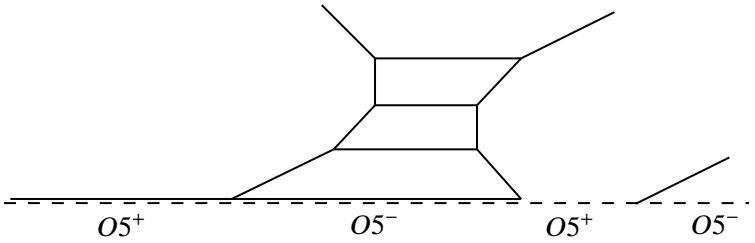

图 3-5 Another equivalent 5-brane web diagram of $SO(7)$ with one spinor

as shown in figure 3-6 (b) and (c). The choices depend on the sign of the mass parameter of the spinor. Nevertheless, we can reduce both of (b) and (c) to figure 3-7 (b) with $O5^-$-plane, with figure (a) being figure 3-7 (a).

Furthermore, we can see how the generalized flop transition acts on the local structure E_2 with $\tilde{O}5$-plane, as depicted in figure 3-7 (c) and (d). And naturally, the flop transition in $\tilde{O}5$-plane background are expected to be equivalent to that in $O5$-plane background.

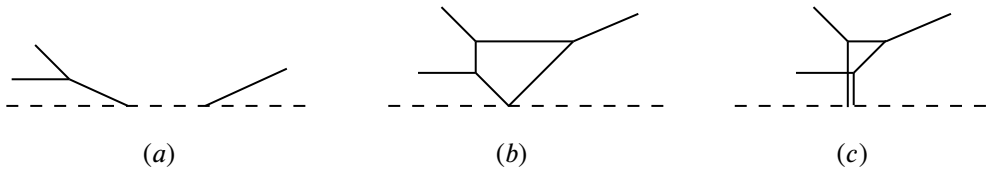

图 3-6 A generalized flop transition for a 5-brane web with an $O5$-plane[2]. Flopping (a) will results in either (b) or (c), and the choice is determined by the sign of the mass parameter.

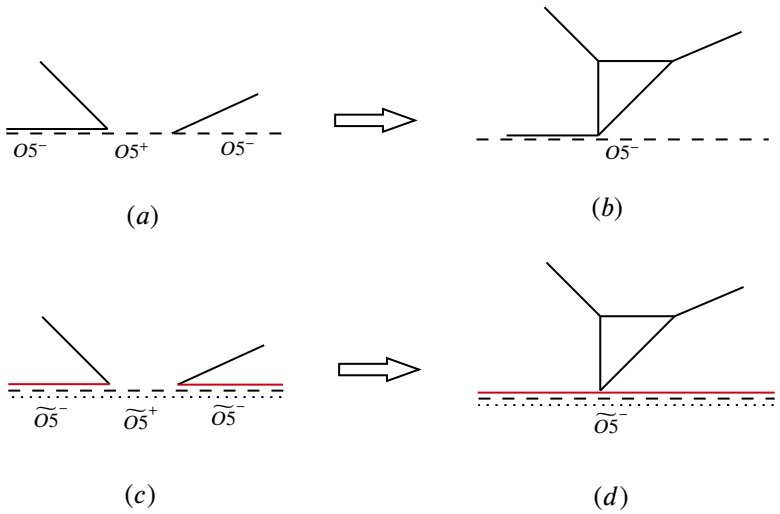

图 3-7 Reduced figures of the generalized flop transition in figure 3-6 in the presence of $O5$-plane or the $\tilde{O}5$-plane.

Appling the flop transition are displayed by the first arrow in figure 3-7 to figure 3-5, once again we obtain an equivalent figure 3-8 (a) for $SO(7)$ with one spinor matter.

We can further transform (a) to (b) by acting two standard flop transitions. The Higgs branch emerges when we put D7-branes at the end of the external parallel $(2,1)$ 5-branes. Then move the D5-brane stretching between D7-branes along the monodromy to infintely far, which implies taking

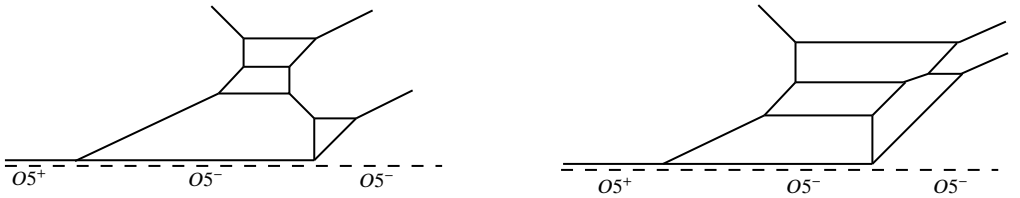

(a)　(b)

图 3-8　(a) An equivalent diagram for $SO(7)$ with one spinor after generalized flop transition acting on figure 3-5. (b) Derived from performing two conventional flop transitions to figure (a).

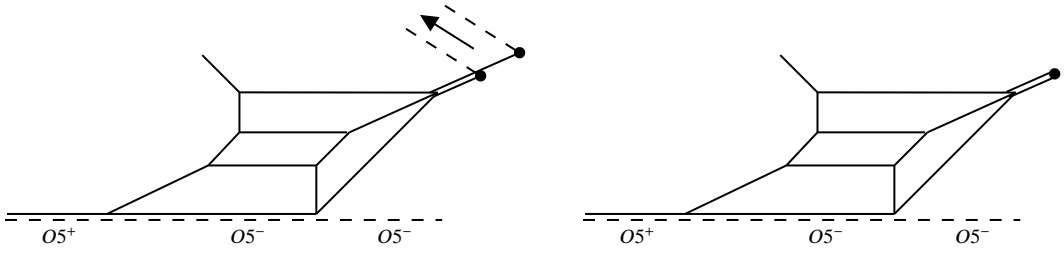

(a)　(b)

图 3-9　(a) Deformation of figure 3-8 (b), with D7-branes put at the end of the parallel external $(2,1)$ 5-branes. (b) 5-brane web diagram for pure G_2 after Higgsing figure (a) and taking to a far infrared limit at the Higgs branch.

a far infrared limit at Higgs branch. The resulting diagram 3-9 (b) describes the pure G_2 gauge theory.

In fact, there is another 5-brane web diagram using $\tilde{O}5$-plane for pure G_2, which results from applying the same Higgsing procedure to figure3-4 (b). And there is only one half D5-brane stretching between the $(2,1)$ 5-brane and $(1,1)$ 5-brane, as shown below.

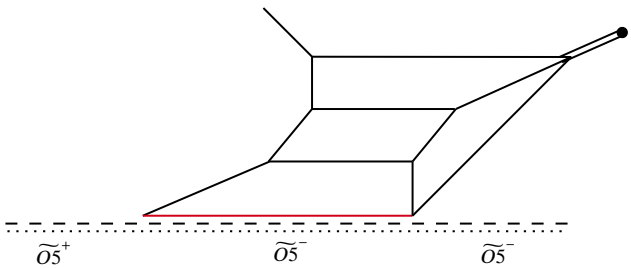

图 3-10　Another 5-brane web diagram with $\tilde{O}5$-plane for pure G_2. Derived from figure3-4 (b) by the same Higgsing process.

3.2　From $SO(8)$ gauge theory with one spinor and one conjugate spinor

This section proposes another approach to derive the 5-brane web diagram for G_2 gauge theories, based on the triality of $SO(8)$ gauge theory in 5d. The triality supports the equivalence of $SO(8)$ plus one vector and one spinor and $SO(8)$ plus one spinor and one conjugate spinor. Recall

that we derived the 5-brane diagram for pure $SO(7)$ from $SO(8)$ with one flavor in vector representation by Higgsing, and then Higgsing $SO(7)$ plus one spinor produced pure G_2. It indicates that if we start from the diagram for $SO(8)$ with one spinor and one conjugate spinor, we are expected to obtain the 5-brane diagram for pure G_2 theories by Higgsing twice. As shown in the formula 3.1 below, where V denotes vector, and S denotes spinor, $\bar{S}$ denotes conjugate spinor.

$$\begin{array}{ccccc} SO(8)+1V+1S & \overset{Higgsing}{\longrightarrow} & SO(7)+1S & \overset{Higgsing}{\longrightarrow} & G_2 \\ \updownarrow & & & & \\ SO(8)+1\bar{S}+1S & \overset{Higgsing}{\longrightarrow} & SO(7)+1S & \overset{Higgsing}{\longrightarrow} & G_2 \end{array} \tag{3.1}$$

A spinor can be introduced to the brane diagram with $O5$-plane for pure $SO(8)$ by the coupling with $Sp(0)$. While a conjugate spinor has an opposite chirality, and it will result in a discrete theta angle $\theta = \pi$ in the 5-brane diagram for $Sp(0)$. However, the 5-brane web diagram with $O5$-plane succeeds in describing the $Sp(2N)$ in the $\theta = 0$ case, but fails to describe the $\theta = \pi$ case distinctively[2]. Moreover, the 5-brane web construction with $\tilde{O}5$-plane also appears to produce the $Sp(2N)+1F$, but not the pure $Sp(2N)$ theories[10].

To describe $SO(8)$ with one vector and one spinor, we draw a 5-brane web diagram with $O5$-plane depicting a quiver $Sp(0)-SO(8)-Sp(0)$ in figure 3-11. Although the difference in theta angle does not show up in this diagram, the generalized flop transition can manifest this difference to a large extent. The two generalized flop displayed in figure 3-12. So acting these flop transitions respectively to the conjugate spinor and the spinor, we get the deformed 5-brane web diagram 3-13 (a). Also the generalized flop transitions 3-6 mentioned before can yield an equivalent diagram (b), with the spinor and the conjugate spinor represented in different ways.

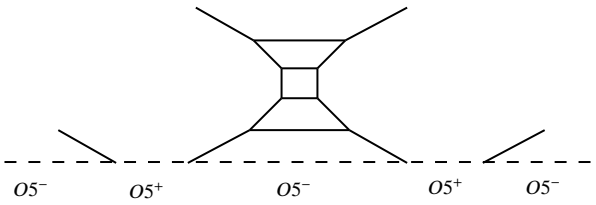

图 3-11 The 5-brane web diagram describing $SO(8)$ with one vector and one spinor, forms a quiver $Sp(0)-SO(8)-Sp(0)$.

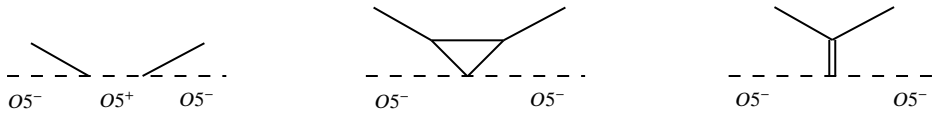

图 3-12 Two kinds of the generalized flop transition for the 5-brane diagram including $O5$-plane: 1. (a) → (b), 2. (a) → (c). The two choices depends on the theta angle $\theta = 0$ or π.

Applying two standard flop transitions to the right part of figure 3-13 turns out to be figure 3-14 (a). The following Higgsing procedures are almost in the same fashion as that in subsection

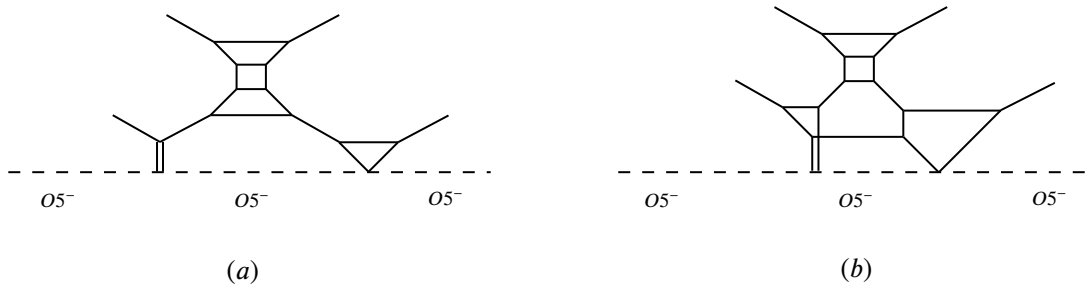

图 3-13 (a) Obtained from performing the generalized flop transitions in figure 3-12. (b) Obtained from performing the generalized flop transitions in figure 3-6. In fact (a) and (b) are equivalent.[2]

3.1. First, put the black dot which denotes the D7-brane to the end of the semi-infinite D5-brane , then perform the Higgsing, and subsequently, take a far-infrared limit. The resulting figure 3-14 (b) should describe $SO(7)$ with one spinor according to the arrow diagram 3.1.

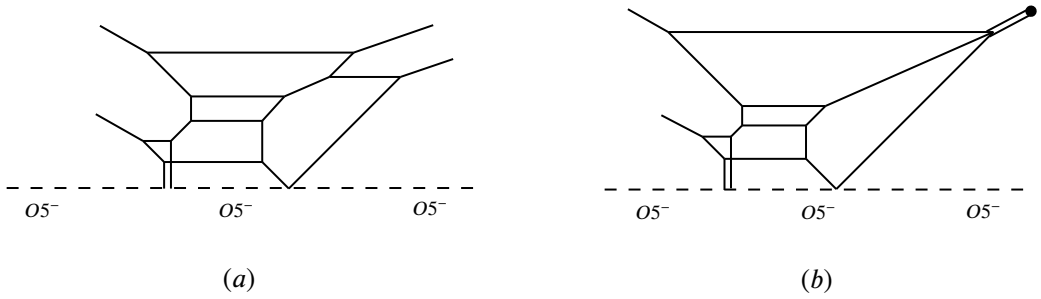

图 3-14 (a) Obtained from applying two standard flop transitions to figure 3-13 (b). (b) Obtained from Higgsing (a), and it depicts $SO(7) + 1S$ according to 3.1.

Aimed to obtain the 5-brane web diagram for pure G_2 , we need once more Higgsing. It implies that we should execute the same operations to the left part of diagram 3-14 (b) since there are two external parallel D5-branes as well. As a consequence, we derive figure 3-15 which could describe the pure G_2 gauge theories.

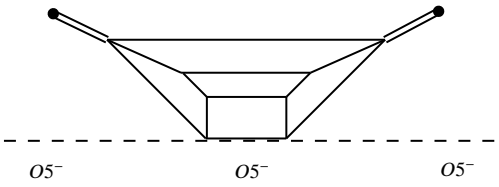

图 3-15 Another 5-brane web diagram for G_2 gauge theories.

3.3 Dualities involving G_2 gauge theories

3.3.1 Effective prepotential of the 5-brane diagrams for pure G_2

Given a gauge group G in 5d gauge theory, its effective prepotential can be computed by[3, 11, 12]

$$\mathcal{F}(\phi) = \frac{1}{2}m_0 h_{ij}\phi_i\phi_j + \frac{\kappa}{6}d_{ijk}\phi_i\phi_j\phi_k + \frac{1}{12}\Big(\sum_{r\in\text{roots}}|r\cdot\phi|^3 - \sum_f\sum_{w\in R_f}|w\cdot\phi + m_f|^3\Big), \tag{3.2}$$

in general. The first two terms are the classical prepotential along the Coulomb branch, where m_0 is the inverse of the squared gauge coupling, ϕ_i denotes the Coulomb branch moduli, and κ is the classical Chern-Simons level. We also have $h_{ij} = \mathrm{Tr}(T_i T_j)$ and $d_{ijk} = \frac{1}{2}\mathrm{Tr}(T_i\{T_j, T_k\})$, with T_i the Cartan generators of the Lie algebra of G. The last two terms represent the quantum contribution of the massive vector multiplet and the matter multiplet respectively[11, 12]. m_f is the mass parameter for hypermultiplets in the representation R_f of the gauge group G. r are the roots of G and w are the weights of the representation R_f.

Initially, let us consider the 5-brane web diagram for pure G_2 3-9 in section 3.1, which is derived from $SO(7)$ with one spinor by Higgsing. We use the Dynkin basis to parameterize the Coulomb branch moduli ϕ_i, then the prepotential for the pure G_2 gauge theories without matter turns out to be

$$\mathcal{F}_{G_2}(\phi) = m_0(\phi_1{}^2 - 3\phi_1\phi_2 + 3\phi_2{}^2) + \frac{4}{3}\phi_1{}^3 - 4\phi_1{}^2\phi_2 + 3\phi_1\phi_2{}^2 + \frac{4}{3}\phi_2{}^3, \tag{3.3}$$

Taking the derivative with respect to the Coulomb branch moduli ϕ_1 and ϕ_2, we can obtain the monopole tension

$$\frac{\partial\mathcal{F}_{G_2}}{\partial\phi_1} = (m_0 + 2\phi_1 - \phi_2)(2\phi_1 - 3\phi_2), \tag{3.4}$$

$$\frac{\partial\mathcal{F}_{G_2}}{\partial\phi_2} = (-\phi_1 + 2\phi_2)(3m_0 + 4\phi_1 + 2\phi_2). \tag{3.5}$$

The monopoles in 5d gauge theory can be realized by the D3-branes wrapping a face in the 5-brane webs. This implies that the monopole tension given by (3.5) can be written as a linear combination of the area of faces. The 5-brane web diagram for G_2 is naturally divided into four faces, which are bounded by D5-branes. At this stage, we are inspired to parameterize the Coulomb branch moduli in the orthogonal basis $\mathbb{R}^2$, denoted as a_1, a_2. The relation between a_1, a_2 and ϕ_1, ϕ_2 is

$$2\phi_1 - 3\phi_2 = a_2 - a_1, \qquad -\phi_1 + 2\phi_2 = a_1. \tag{3.6}$$

In the 5-brane web diagram for pure G_2 3-16, a_1 and a_2 can be expressed as the heights of the bottom two D5-branes respectively. m_0 is given by the distance of the external (2, 1) 5-brane and the external $(1, -1)$ 5-brane on the $\tilde{O}5$-plane.

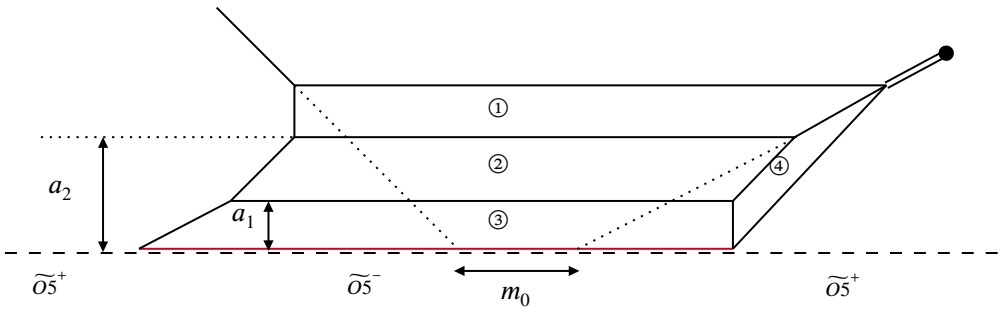

图 3-16 5-brane web diagram for pure G_2 derived from Higgsing $SO(7)$ with one spinor. a_1, a_2 are the Coulomb branch moduli and m_0 is the inverse of the gauge coupling constant.

From figure 3-16 we can easily analyze that ① and ③ are exactly congruent. Then the distance between the top two D5-branes is a_1, and the lengths of the four parallel D5-branes are $3a_2+3a_1+m_0$,

$3a_2 + a_1 + m_0$, $3a_2 + a_1 + m_0$, $3a_2 + 3a_1 + m_0$ respectively from top to bottom. Hence the area of the four faces is

$$① = a_1(3a_2 + 2a_1 + m_0), \tag{3.7}$$

$$② = (a_2 - a_1)(3a_2 + a_1 + m_0), \tag{3.8}$$

$$③ = a_1(3a_2 + 2a_1 + m_0), \tag{3.9}$$

$$④ = a_1 a_2. \tag{3.10}$$

An qualitative explanation can be given to these results. Recall the whole process from $SO(7)$ with one spinor to G_2, ① and ④ got connected during Higgsing. While ③ and ④ become connect through the generalized flop transition. ③ should be doubled because of the reflection symmetry of $\tilde{O}5$-plane.

Comparing with the monopole tension (3.5) and using the basis relations (3.6), we finally reach to

$$\frac{\partial \mathcal{F}_{G_2}}{\partial \phi_1} = ② = (a_2 - a_1)(3a_2 + a_1 + m_0) \tag{3.11}$$

$$\frac{\partial \mathcal{F}_{G_2}}{\partial \phi_2} = ① + 2 \times ③ + ④ = a_1(10a_2 + 6a_1 + 3m_0). \tag{3.12}$$

Next we will study the other 5-brane web diagram 3-17, which is obtained after Higgsing $SO(8)$ with one spinor and one conjugate spinor twice. In the same fashion, we label the five faces of this

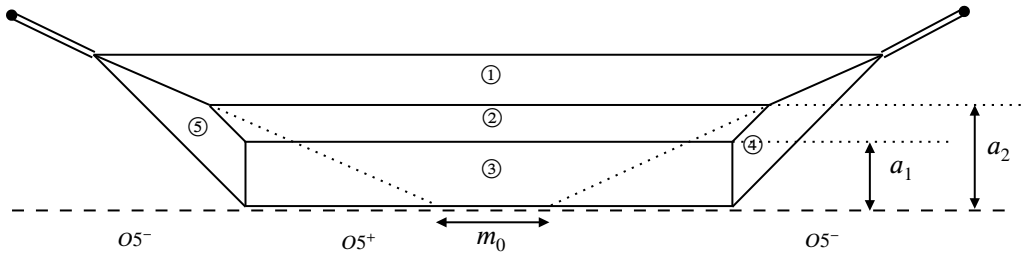

图 3-17　Another 5-brane web diagram with $O5^-$-plane for pure G_2. We constructed it using the triality of $SO(8)$ gauge theory in section 3.2.

5-brane web diagram. a_1, a_2 still denote the height of the lower two D5-branes and m_0 denotes the distance of the two external 5-branes on the $O5^-$-plane. Therefore the lengths of the four horizontal D5-branes are $4a_1+4a_2+m_0$, $4a_2+m_0$, $2a_1+2a_2+m_0$, $2a_1+2a_2+m_0$ from top to bottom respectively. Their area is given by

$$① = a_1(4a_2 + 2a_1 + m_0) \tag{3.13}$$

$$② = (a_2 - a_1)(3a_2 + a_1 + m_0) \tag{3.14}$$

$$③ = a_1(2a_2 + 2a_1 + m_0) \tag{3.15}$$

$$④ = a_1 a_2 \tag{3.16}$$

$$⑤ = a_1 a_2. \tag{3.17}$$

We find that

$$\frac{\partial \mathcal{F}_{G_2}}{\partial \phi_1} = ② = (a_2 - a_1)((3a_2 + a_1 + m_0), \tag{3.18}$$

$$\frac{\partial \mathcal{F}_{G_2}}{\partial \phi_2} = ① + 2 \times ③ + ④ + ⑤ = a_1(10a_2 + 6a_1 + 3m_0), \tag{3.19}$$

Also, an qualitative explanation is that the two Higgsing procedures of $SO(8)$ with one spinor and one conjugate spinor made the regions ①, ②, ③, ④, ⑤ connected. ③ should be doubled as well due to the reflection symmetry of the $O5$-plane.

3.3.2 Duality between pure G_2 and pure $SU(3)$

The 5-brane web diagram for pure G_2 in figure 3-18 (a) has a different notation for the monodromy branch cut of D7-brane. The monodromy extends toward the right direction, instead of the left as introduced in subsection 3.1. It's useful to change the notation since it will be more convenient to calculate the area of the faces, even when it is transformed to the 5-brane web diagram of pure $SU(3)$ with the Chern-Simons(CS) level 7 by taking the S-duality. The S-duality corresponds to rotate figure 3-18 by $\pi/2$, the resulting diagram is shown in figure 3-18 (b). Note that the $\tilde{O}5$-plane becomes an $\tilde{O}N$-plane in (b). In terms of geometry, the S-duality can be understood as the fiber-base duality.

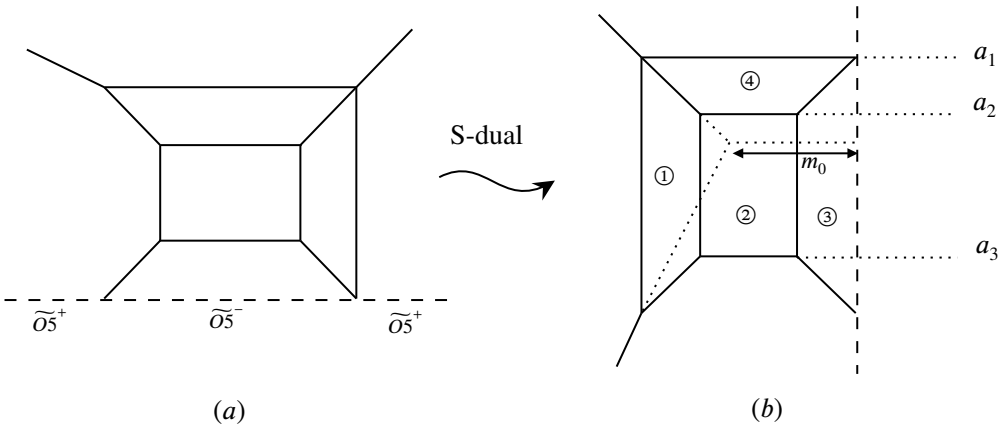

图 3-18 (a) The 5-brane web diagram for pure G_2 gauge theory. The monodromy branch cut of D7-brane extends to right direction instead of left direction in subsection 3.1. (b) The 5-brane web diagram for pure $SU(3)$ with the Chern-Simons(CS) level 7, which is S-dual to the G_2 diagram.

We labeled the faces of figure 3-18 (b) and parameterized it with the inverse of the squared gauge coupling m_0, and the Coulomb branch moduli of $SU(3)$, i.e. a_1, a_2, a_3. Note that $a_1 + a_2 + a_3 = 0$. The area of the faces can be expressed as

$$① = (a_1 - a_2)(a_1 - a_3), \tag{3.20}$$

$$② = (a_2 - a_3)(2a_2 - a_1 + m_0), \tag{3.21}$$

$$③ = (a_1 - a_2)(a_1 - a_3), \tag{3.22}$$

$$④ = (a_1 - a_2)(a_2 + m_0). \tag{3.23}$$

According to the general equation (3.2), the prepotential of $SU(3)$ gauge group is given by

$$\begin{aligned}\mathcal{F}_{SU(3)_7} &= \frac{m_0}{2}(a_1^2+a_2^2+a_3^2)+\frac{1}{6}((a_1-a_2)^3+(a_1-a_3)^3+(a_2-a_3)^3)+\frac{7}{6}(a_1^3+a_2^3+a_3^3)\\ &= m_0(\phi_1^2-\phi_1\phi_2+\phi_2^2)+\frac{4}{3}\phi_1^3+3\phi_1^2\phi_2-4\phi_1\phi_2^2+\frac{4}{3}\phi_2^3.\end{aligned} \tag{3.24}$$

where the Coulomb branch moduli ϕ_1, ϕ_2 are the Dynkin basis, while a_1, a_2, a_3 are the orthogonal basis of $\mathbb{R}^3$. The Coulomb branch modulus in different basis have the relation

$$a_1=\phi_1,\quad a_2=-\phi_1+\phi_2,\quad a_3=-\phi_2. \tag{3.25}$$

And it satisfies the condition $a_1+a_2+a_3=0$ naturally. Then the monopole tension can be derived by taking derivatives

$$\frac{\partial\mathcal{F}_{SU(3)_7}}{\partial\phi_1}=(2\phi_1-\phi_2)(m_0+2\phi_1+4\phi_2), \tag{3.26}$$

$$\frac{\partial\mathcal{F}_{SU(3)_7}}{\partial\phi_2}=(-\phi_1+2\phi_2)(m_0-3\phi_1+2\phi_2). \tag{3.27}$$

Subsequently, we compare the tension which is dependent on a_1, a_2, a_3 to the area of the faces, and obtain

$$\frac{\partial\mathcal{F}_{SU(3)_7}}{\partial\phi_1}=①+④+2\times③=(a_1-a_2)(3a_1+a_2-3a_3+m_0), \tag{3.28}$$

$$\frac{\partial\mathcal{F}_{SU(3)_7}}{\partial\phi_2}=②=(a_2-a_3)(2a_2-a_1+m_0). \tag{3.29}$$

Eventually, we derive the same relation between monopole tension and the area of faces as that in the G_2 case. The Chern-Simons level is the third derivative of the prepotential. This equation set (3.29) also indicates the Chern-Simons level of the 5-brane web diagram for pure $SU(3)$ is 7.

Furthermore, we can study the explicit duality map between the parameters of these two gauge theories, just from the geometry of the 5-brane web diagrams

$$m_0^{SU(3)_7}=-\frac{m_0^{G_2}}{3}, \tag{3.30}$$

$$\phi_1^{SU(3)_7}=\phi_2^{G_2}+\frac{1}{3}m_0^{G_2}, \tag{3.31}$$

$$\phi_2^{SU(3)}=\phi_1^{G_2}+\frac{2}{3}m_0^{G_2}. \tag{3.32}$$

第 4 章　5D Nekrasov Partition Functions for G_2 Gauge Theories

4.1　Topological vertex formalism with $O5$-plane

The topological vertex formalism serves as an efficient and well-known method to systematically compute the topological string partition function of a toric Calabi-Yau threefolds[13]. There exists a correspondence between the toric diagram and the (p, q) 5-brane web diagram in type IIB string theory[14, 15], which enables us to establish a similar formalism on a (p, q) 5-brane web diagram. While for non-toric Calabi-Yau geometry, we can extend the topological vertex formalism for the corresponding 5-brane web diagram by tuning Kähler parameters properly.

The topological vertex $C_{\lambda_1\lambda_2\lambda_3}$ is labeled by the Young diagrams $\lambda_1, \lambda_2, \lambda_3$ that are assigned to the legs of the considering trivalent vertex in a clockwise direction.

$$C_{\lambda_1\lambda_2\lambda_3} = q^{\frac{\kappa(\lambda_2)}{2}+\frac{\kappa(\lambda_3)}{2}} s_{\lambda_3}(q^{-\rho}) \sum_{\nu} s_{\lambda_1^t/\nu}(q^{-\rho-\lambda_3}) s_{\lambda_2/\nu}(q^{-\rho-\lambda_3^t}), \tag{4.1}$$

where $\kappa(\lambda) := 2\sum_{(i,j)\in\lambda}(j-i)$, and $q^{-\rho-\lambda} = \{q^{i-1/2-\lambda_i}\}_{i=1}^{\infty}$ with a sequence $\rho = \{i-1/2\}_{i=1}^{\infty}$. Also, λ^t means the dual Young diagram of λ, and s_λ is the Schur function which is defined as

$$s_\lambda(x_1, \ldots, x_n) := \frac{\det\left(x_i^{\lambda_j+n-j}\right)}{\det\left(x_i^{n-j}\right)}. \tag{4.2}$$

In fact, all the Schur functions form a complete basis of symmetric polynomials, and the skew-Schur function $s_{\lambda/\nu}$ is defined as a linear combination of Schur functions.

$$s_\mu s_\nu = \sum_\lambda c_{\mu\nu}^\lambda s_\lambda, \quad s_{\lambda/\mu} := \sum_\nu c_{\mu\nu}^\lambda s_\nu. \tag{4.3}$$

In the topological string partition functions, the topological vertices are weighted by both the framing factors and Kähler parameters for the internal lines. Here the framing factor associated to each internal line is defined by both the Young diagrams assigned to the line and the local geometry around this line.

Given the local geometry around the internal line assigned by λ:

The framing factor associated to the internal line λ is defined by f_λ^{bc-ad}, where

$$f_\lambda := (-1)^{|\lambda|} q^{\frac{\kappa(\lambda)}{2}}. \tag{4.4}$$

Here $|\lambda|$ is the number of boxes in Young diagram λ, and the power $bc - ad$ comes from the wedge product the slopes of the two legs, which also means the (p, q) charge of the adjacent 5-branes. The framing factor obeys $f_\lambda f_{\lambda^t} = 1$.

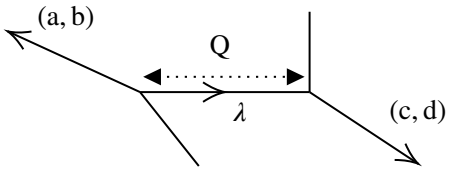

图 4-1　The internal line is assigned by λ, and the slope of the external lines are respectively (a, b) and (c, d).

The Kähler parameter is denoted by Q in the diagram above. And it is the exponentiated length of the 5-branes. Therefore we can introduce the edge factor $(-Q)^{|\lambda|} f_\lambda^{bc-ad}$ to the line assigned by λ.

Finally, the topological string partition function of the 5-brane web diagram is computed by taking products of all the factors and summing over all possible Young diagrams:

$$Z = \sum_{\lambda,\mu,\nu\ldots} \prod(\text{Edge factor}) \prod(\text{Vertex factor}) \tag{4.5}$$

When the case extends to 5-brane web diagrams with $O5$-planes, we have the generalized topological vertex formalism[16] accordingly. Firstly, let us consider the following 5-brane diagram with the Kähler parameter Q', which can be seen as the pure "$Sp(0)$" gauge theory. So it is trivial indeed. Applying the generalized flop transition 3-12 to deform diagram 4-2 and change the Kähler

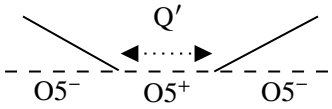

图 4-2　A trivial 5-brane diagram with $O5$-plane which depicts "$Sp(0)$".

parameter Q' to $Q = Q'^{-1}$, we obtain the left diagram of 4-3 below。

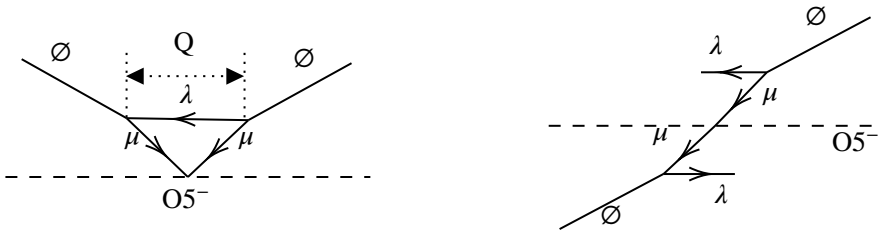

图 4-3　Deformed trivial 5-brane diagram with $O5$-plane and the strip diagram after reflection

So reflecting half of this diagram with respect of the $O5$-plane yields the diagram on the right. Notice that the Young diagrams λ, μ assigned to the internal legs will become their dual diagrams λ^t, μ^t in its mirror image part, which also means that we have to the reverse the direction of the arrows if we still assign them with the original Young diagrams λ, μ.

Now we need to compute the new framing factor associated to the mirror image since the direction of the edges will change, and the order of Young diagrams in the topological vertices should be reversed from clockwise ordering to counter-clockwise ordering after reflection. Assuming the new framing factor is determined only by the Young diagrams of the gluing legs, i.e. the horizontal lines in the diagram below. Denote it by g_λ. And we can derive its expression by utilizing the

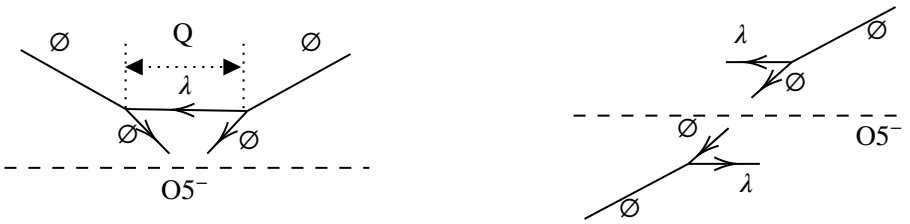

图 4-4 Local diagrams of the trivial 5-brane diagram with $O5$-plane and its equivalent strip diagram

equivalence of the two diagrams and applying the conventional topological vertex formalism. For convenience, we assign all the external legs with trivial Young diagrams. So applying the topological vertex formalism to both the diagrams. we obtain two equivalent formulae to describe these diagrams

$$(-Q^2)^{|\lambda|} f_\lambda^3 C_{\varnothing\varnothing\lambda} C_{\varnothing\varnothing\lambda^t} = (-Q^2)^{|\lambda|} f_\lambda^3 s_\lambda(q^{-\rho}) s_{\lambda^t}(q^{-\rho}), \tag{4.6}$$

$$(-Q^2)^{|\lambda|} g_\lambda C_{\varnothing\varnothing\lambda} C_{\varnothing\varnothing\lambda} = (-Q^2)^{|\lambda|} g_\lambda f_\lambda^2 s_\lambda(q^{-\rho}) s_\lambda(q^{-\rho}). \tag{4.7}$$

Using the identity

$$s_{\lambda^t}(q^{-\rho}) = (-1)^{|\lambda|} f_\lambda s_\lambda(q^{-\rho}), \tag{4.8}$$

thus $g_\lambda = (-1)^{|\lambda|} f_\lambda^2$. It also indicates that

$$C_{\varnothing\varnothing\lambda^t} = (-1)^{|\lambda|} f_\lambda^{-1} C_{\varnothing\varnothing\lambda}, \tag{4.9}$$

which can be extended to a more general case where the vertex is associated to three internal lines

$$C_{\mu\nu\lambda} = (-1)^{|\mu^t|}(-1)^{|\nu^t|}(-1)^{|\lambda^t|} f_{\mu^t}^{-1} f_{\nu^t}^{-1} f_{\lambda^t}^{-1} C_{\mu^t\nu^t\lambda^t}. \tag{4.10}$$

Note that the relation between the vertices here is actually the same as that given in the reference[3] (4.3) but it uses the different notation of the framing factor $f_\lambda = (-1)^{|\lambda|} q^{\frac{1}{2}(||\lambda^t||^2 - ||\lambda||^2)}$ with $||\lambda||^2 = \sum_i \lambda_i^2$. Since $||\lambda^t||^2 - ||\lambda||^2 = 2\sum_{(i,j)\in\lambda}(i-j)$, then $f_\lambda = (-1)^{|\lambda|} q^{\sum_{(i,j)\in\lambda}(i-j)} = (-1)^\lambda q^{-\kappa(\lambda)/2}$, which is exactly the inverse of the framing factor defined in (4.4).

Back to the case where the external legs are all trivially assigned, we shall use this new framing factor when applying the topological vertex formalism to the right diagram of 4-3. So its partition function is given by:

$$Z(Q) = \sum_{\mu,\lambda} (-Q^2)^{|\mu|}(-Q^2)^{|\lambda|}(-1)^{|\lambda|} f_\lambda^2 C_{\varnothing\mu\lambda} C_{\varnothing\mu^t\lambda} \tag{4.11}$$

Substituting the vertex factors and the framing factor by (4.1) and (4.4), and utilizing the Cauchy identity

$$\begin{aligned} &\sum_\lambda (-Q)^{|\lambda|} s_{\lambda/\mu^t}(q^{-\rho-\sigma}) s_{\lambda^t/\nu}(q^{-\rho-\tau}) \\ &= P.E.(-\frac{q}{(1-q)^2}Q) N_{\sigma^t\tau}(Q,q) \cdot \sum_\eta (-Q)^{|\mu|+|\nu|-|\eta|} s_{\nu^t/\eta}(q^{-\rho-\sigma}) s_{\mu/\eta^t}(q^{-\rho-\tau}), \end{aligned} \tag{4.12}$$

which also implies a more useful identity

$$N_{\lambda\lambda}^{-1} = (-1)^{|\lambda|} s_\lambda(q^{-\rho}) s_{\lambda^t}(q^{-\rho}), \tag{4.13}$$

we obtain

$$Z(Q) = P.E.(-\frac{q}{(1-q)^2}Q^2)\sum_{\lambda}(Q^2)^{|\lambda|}f_{\lambda}^3\frac{N_{\lambda\lambda^t}(Q^2,q)}{N_{\lambda\lambda}(1,q)}. \tag{4.14}$$

The Nekrasov factor in the unrefined limit is

$$N_{\lambda\nu}(Q,q) := \prod_{(i,j)\in\lambda}(1-Qq^{\lambda_i+\nu_j^t-i-j+1})\prod_{(i,j)\in\nu}(1-Qq^{-\nu_i-\lambda_j^t+i+j-1}), \tag{4.15}$$

and the P.E. function is

$$P.E.(f(x_1,x_2,\ldots,x_n)) := \exp\left(\sum_{k=1}^{\infty}\frac{1}{k}f(x_1^k,x_2^k,\ldots,x_n^k)\right). \tag{4.16}$$

Now we can see that the partition function (4.14) merely depends on the Young diagram λ, which implies the fusion rule at the vertex. Computing the formula (4.14) as series expansions of Kähler parameters we will get

$$Z(Q) = 1 + \mathcal{O}(Q^{11}) \tag{4.17}$$

Note that this is the partition function for $Sp(0)$, so it should be trivial, namely

$$Z(Q) = 1 \tag{4.18}$$

Thus we can see the efficiency of deriving partition functions by the topological vertex formalism.

4.2 Partition function for pure G_2 from O-vertex method

Since the trivalent vertex can be described by the vertex factor with three Young diagrams assigned to the edges, it's natural to think that if we can treat the local structure appearing in figure 4-2 as a special type of vertex, especially when the edges are internal lines. Generally, there are two types of vertices shown in figure 4-5 below, which we call O-vertex[4]. The solid line denotes the internal line of a web diagram, and it is assigned by a Young diagram ν.

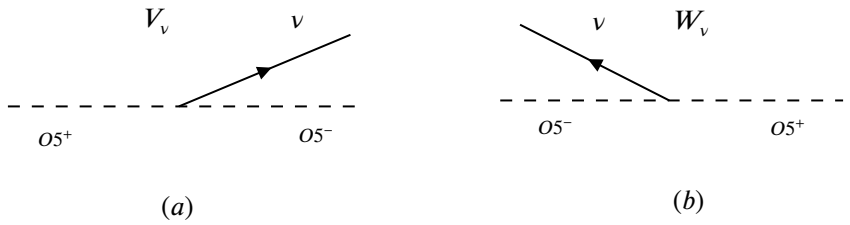

图 4-5　Two types of O-vertices

The way to calculate its contribution to the partition function is similar to that in the last section. For instance, first we bring an external $(2,-1)$ 5-brane assigned by a null Young diagram $\varnothing$ to figure 4-5 (a). This step will cause no difference to the final partition functions. We define the Kähler parameter Q' to be the distance of two 5-branes on an $O5$-plane, and P' to be the height of the internal line. Second, perform a generalized flop transition (a)→(b) in figure 3-7 to the diagram to obtain figure 4-6 (b). The parameters P and Q in figure (b) satisfy $Q' = Q^{-1}$ and $P' = PQ$. The partition function can be easily written according to the topological vertex formalism in the last

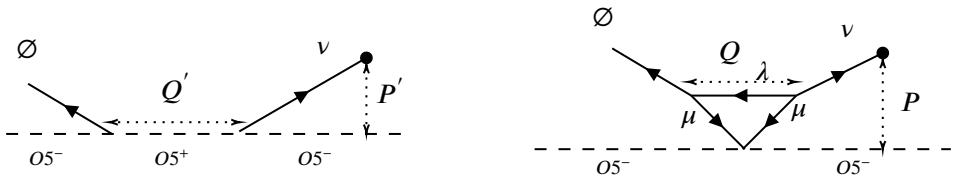

(a) (b)

图 4-6 Applying a generalized flop transition

section. Then the vertex function V_ν is defined by the partition function of this local structure after taking limit $Q \to \infty$ with PQ fixed.

$$\begin{aligned} \lim_{Q\to\infty} Z_\nu(P,Q) &= \sum_{\substack{\mu,\lambda \\ 2|\mu|+2|\lambda|=|\nu|}} (-Q^2)^{|\mu|} Q^{2|\lambda|} (-P)^{|\nu|} f_\lambda^2 C_{\nu\mu\lambda} C_{\varnothing\mu^t\lambda} \\ &\propto \sum_{\substack{\mu,\lambda \\ 2|\mu|+2|\lambda|=|\nu|}} (-1)^{|\mu|} f_\lambda^2 C_{\nu\mu\lambda} C_{\varnothing\mu^t\lambda} := V_\nu. \end{aligned} \tag{4.19}$$

Substituting the expression for framing factor and vertex factors, we can rewrite it in a more brief form,

$$V_\nu = \frac{P_\nu(q)}{(q;q)_{|\nu|/2}}, \tag{4.20}$$

where $(q;q)_n = \prod_{k=0}^{n-1}(1-q^{k+1})$ and P_ν is a polynomial of q with the highest order power $|\nu|(|\nu|+2)/8$. Likewise, the vertex function W_ν for figure 4-5 (b) is $W_\nu = \tilde{P}_\nu(q)/(q;q)_{|\nu|/2}$. The explicit expression of P_ν and $\tilde{P}_\nu$ are given in the reference[4].

Now consider the 5-brane web diagram for pure G_2 in section 3.1, which results from Higgsing $SO(7)$ with one spinor. The first diagram in 4-7 is exactly figure 3-9 (b), with Kähler parameters associated to the internal lines.

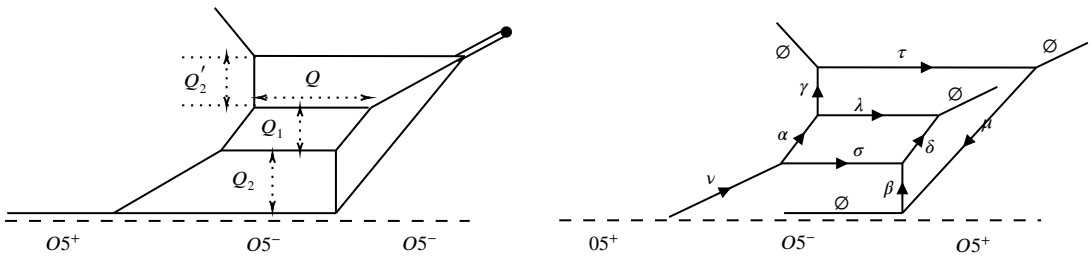

(a) (b)

图 4-7 (a) The 5-brane web diagram for pure G_2 from the second diagram in figure 3-9. The Kähler parameters associated to the internal lines are marked in the diagram. (b) Assign Young diagrams to each edges. Especially, the four external lines are assigned with an empty Young diagram.

Since the Kähler parameter is related to the length of the edges. So $Q_2' = Q_2$ for their corresponding edges have the same length. Recall the Coulomb branch moduli in figure 3-16. We define

$A_1 = e^{-a_1}$ and $A_2 = e^{-a_2}$, and also

$$Q_1 = e^{a_1 - a_2} = A_1^{-1} A_2, \tag{4.21}$$

$$Q_2 = e^{-a_1} = A_1, \tag{4.22}$$

$$Q = e^{-a_1 - 3a_2 - m_0}. \tag{4.23}$$

Moreover, the instanton fugacity $\mathfrak{q}$ is defined as

$$\mathfrak{q} = e^{-m_0} = Q Q_1^{-3} Q_2^{-4}. \tag{4.24}$$

The second diagram in figure 4-7 have Young diagrams mark each lines. All the semi-infinite D5-branes or those with one end on D7-brane will correspond to the external lines, which should be assigned with empty Young diagram $\varnothing$. Accordingly, the partition function for pure G_2 can be read from diagram 3.1 (b).

$$\begin{aligned} Z_{G_2} = \sum_{\alpha,\beta,\gamma,\delta,\lambda,\mu,\nu,\sigma,\tau} & (-Q_1)^{|\alpha|+|\delta|}(-Q_2)^{|\nu|+|\gamma|+|\beta|}(-Q_1Q_2^2)^{|\mu|}(-Q)^{|\lambda|+|\sigma|}(QQ_2^2)^{|\tau|} \\ & f_\alpha^{-1} f_\gamma^{-1} f_\mu f_\beta f_\sigma f_\lambda^{-1} f_\delta^{-1} f_\tau^{-3} V_\nu C_{\nu^t \alpha\sigma} C_{\alpha^t \gamma\lambda} C_{\gamma^t \varnothing\tau} C_{\mu\tau^t\varnothing} C_{\beta\mu^t\varnothing} C_{\delta\beta^t\sigma^t} C_{\delta^t\lambda^t\varnothing} \end{aligned} \tag{4.25}$$

The instanton partition function is derived from the full partition function with the perturbative part removed.

$$Z_{inst} = \frac{Z_{G_2}}{Z_{pert}} = \sum_k Z_k \mathfrak{q}^k, \tag{4.26}$$

where Z_k is the k-instanton partition function. Since Q is proportional to $\mathfrak{q}$, we extrapolate that the total number of three Young diagrams $|\lambda|+|\sigma|+|\tau|$ indicates the order of the terms. In other words, to compute Z_k, we should fix $|\lambda| + |\sigma| + |\tau|$ to be k.

The perturbative part results from Z_{G_2} taking the limit $Q \to 0$, which is exactly the 0-instanton partition function Z_0.

$$\begin{aligned} Z_{pert} =& \lim_{Q\to 0} Z_{G_2} \\ \approx& P.E.\left(\frac{2q}{(1-q)^2}(Q_1 + Q_2 + Q_1Q_2 + Q_1Q_2^2 + Q_1Q_2^3 + Q_1^2Q_2^3)\right) \\ =& P.E.\left(\frac{2q}{(1-q)^2}(A_1^{-1}A_2 + A_2 + A_1 + A_1A_2 + A_1^2A_2 + A_1A_2^2)\right). \end{aligned} \tag{4.27}$$

Substituting the expressions for factors and using the Cauchy identity to simplify the results, we obtain a formula for Z_{inst}, which is more convenient to compute[17]

$$\begin{aligned} Z_{inst} = \sum_{\lambda,\sigma,\tau} & Q^{|\lambda|+|\sigma|}(QQ_2^2)^{|\tau|} f_\sigma f_\lambda^{-1} f_\tau^{-2} N_{\lambda\lambda}^{-1}(1,q) N_{\sigma\sigma}^{-1}(1,q) N_{\tau\tau}^{-1}(1,q) \\ & N_{\sigma\lambda}(Q_1,q)^{-2} N_{\sigma\tau}(Q_1Q_2,q)^{-1} N_{\lambda\tau}(Q_2,q)^{-1} N_{\varnothing\sigma}(Q_2,q)^{-1} \\ & N_{\tau^t\varnothing}(Q_1Q_2^2,q)^{-1} N_{\varnothing\lambda}(Q_1Q_2,q)^{-1} N_{\tau^t\sigma}(Q_1Q_2^3,q)^{-1} N_{\tau^t\lambda}(Q_1^2Q_2^3)^{-1} \\ & M_{\sigma\lambda\tau}(Q_2, Q_1Q_2, Q_1Q_2^2), \end{aligned} \tag{4.28}$$

where M-factor is given by

$$M_{\lambda^{(1)},\ldots,\lambda^{(N)}}(X_1,\ldots,X_N) = \frac{\prod_{s=1}^N \prod_{(i,j)\in\lambda^{(s)}} (1 - X_s^2 q^{i-j-\lambda_i^{(s)}+(\lambda^{(s)})_j^t})}{\prod_{1\le s<r\le N} \prod_{(i,j)\in\lambda^{(s)}} (1 - X_s X_r q^{i+j-1-\lambda_i^{(s)}-\lambda_j^{(r)}}) \prod_{(m,n)\in\lambda^{(r)}} (1 - X_s X_r q^{1-m-n+(\lambda^{(s)})_m^t+(\lambda^r)_n^t})} \tag{4.29}$$

4.3 Partition function for pure G_2 by cutting-gluing

In this section, we continue to compute the partition function of another 5-brane web diagram in figure 3-15, using a relatively ingenious approach. And then compare with the instanton partition functions in the last section to check the equality using Mathematica. By doing these, we can see the validity of the O-vertex method, and again the equivalence of the two 5-brane web constructions of pure G_2 theories.

Figure 4-8 (a) is the 5-brane web diagram for pure G_2 from figure 3-15, assigned with Kähler parameters and Young diagrams λ_i. Firstly, we reflect the out-most 5-branes in green with respect to $O5$-plane. Subsequently, we cut the horizontal D5-branes in the middle. Note that the D5-brane on the top of $O5$-plane of the left part has a reverse direction. And this is the only characteristic which distinguish the 5-brane web diagram of G_2 from that for $SU(4)$[18]. Actually it is more understandable when thinking about the diagram before Higgsing, say figure 3-14 (d). If we cut the diagram in the middle first and then reflect the out-most 5-branes of the left part, then the Higgsing will bring the D5-brane of the left part, which is now assigned with λ_0^t, to the $O5$-plane. So the cutting process decomposed the 5-brane web diagram of G_2 into two strip diagrams.

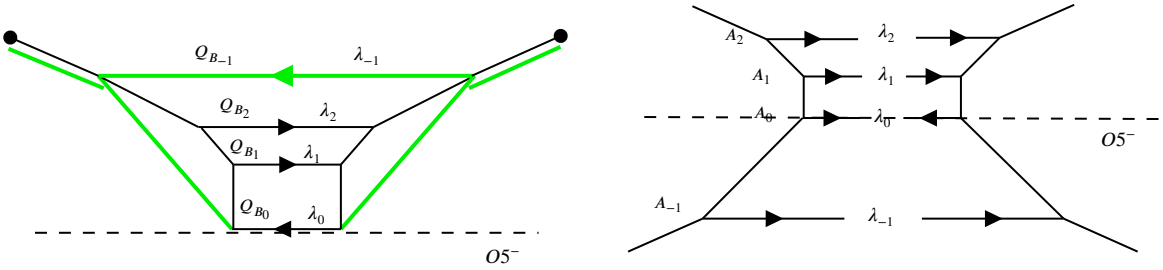

(a) (b)

图 4-8 (a) The 5-brane web diagram for pure G_2 in figure 3-15, assigned with Kähler parameters and Young diagrams. (b) Derived from flipping the out-most 5-branes colored in green and cutting all the D5-branes in the middle.

The strip amplitudes are given by the product of $Z_\lambda(q)$ and $\mathscr{R}_{\mu\nu}$, which are defined as[3, 19]

$$Z_\lambda(q) = \prod_{(i,j)\in\lambda} (1 - q^{\lambda_i+\lambda_j^t-i-j+1}), \tag{4.30}$$

$$\mathscr{R}_{\mu\nu}(Q,q) = \mathscr{M}(Q,q)^{-1} N_{\mu^t\nu}(Q,q), \tag{4.31}$$

where

$$\mathscr{M}(Q,q) = P.E.(\frac{q}{(1-q)^2}Q), \tag{4.32}$$

and the Nekrasov factor $N_{\mu\nu}(Q,q)$ has been introduced in the equation (4.15). The way to parameterize figure 3-15 (a) is the same as figure 3-17. We define $A_0 = 1$, $A_1 = e^{-a_1}$, $A_2 = e^{-a_2}$, $A_{-1} = A_1^{-1}A_2^{-1}$, which is associated to the distance between the D5-brane and the $O5$-plane. Also we introduce a matrix with entries $Q_{ij} = A_i A_j^{-1}, (-1 \le j < i \le 2)$.

To compute the partition function of G_2 gauge theories, we need to glue the two parts in figure 4-8. An extra factor $(-1)^{|\lambda_0|} f_{\lambda_0}^{-1}$ will arise from gluing the D5-branes with opposite directions on

the top of the $O5$-plane, according to the transformation of vertex after reflection (4.10). As before, the instanton fugacity is defined by

$$\mathfrak{q} = e^{-m_0}. \tag{4.33}$$

The Kähler parameters denoted by Q_{B_i} are associated to the lengths of the D5-branes, whose results are already given in subsection 3.2. Therefore

$$Q_{B_0} = Q_{B_1} = \mathfrak{q}A_1^2A_2^2, \quad Q_{B_2} = \mathfrak{q}A_2^4, \quad Q_{B_{-1}} = \mathfrak{q}A_1^4A_2^4. \tag{4.34}$$

Finally, the partition function of pure G_2 described by this construction can be formulated as [3]

$$Z_{G_2} = \sum_{\lambda_i}(-1)^{|\lambda_0|}f_{\lambda_2}^{-3}f_{\lambda_1}^{-1}f_{\lambda_0}^{-1}f_{\lambda_{-1}}^{3}\prod_{i=-1}^{2}(-Q_{B_i})^{|\lambda_i|}Z^{strip1}(\{Q_{ij}\};\lambda_{-1},\lambda_0^t,\lambda_1,\lambda_2)Z^{strip2}(\{Q_{ij}\};\lambda_{-1},\lambda_0,\lambda_1,\lambda_2). \tag{4.35}$$

where Z^{strip1} and Z^{strip2} are the partition functions for the left and right strip diagram in figure 4-8 (b) before gluing. The expressions are given by

$$Z^{strip1}(\{Q_{ij}\};\lambda_{-1},\lambda_0,\lambda_1,\lambda_2) = \prod_{i=-1}^{2}q^{\frac{1}{2}||\lambda_i||^2}\prod_{i=-1}^{2}Z_{\lambda_i}(q)\prod_{-1\le j<i\le 2}\mathscr{R}_{\lambda_i\lambda_j^t}(Q_{ij},q)^{-1}, \tag{4.36}$$

$$Z^{strip2}(\{Q_{ij}\};\lambda_{-1},\lambda_0,\lambda_1,\lambda_2) = \prod_{i=-1}^{2}q^{\frac{1}{2}||\lambda_i^t||^2}\prod_{i=-1}^{2}Z_{\lambda_i}(q)\prod_{-1\le j<i\le 2}\mathscr{R}_{\lambda_i\lambda_j^t}(Q_{ij},q)^{-1} \tag{4.37}$$

To compare the results of partition function of G_2 from different 5-brane diagrams, we can compute their instanton partition functions of the same orders. Recall the equation (4.26), the perturbative part should be removed from the full partition function to derive the instanton partition function. It is obtained by setting the Young diagrams $\lambda_i = \varnothing$ for $i = -1, 0, 1, 2$ and taking the limit $\mathfrak{q} \to 0$. Then only the factors $\mathscr{M}(Q)$ are nontrivial in the full partition function (4.35). More explicitly,

$$Z_{pert} = P.E.(\frac{2q}{(1-q)^2}(A_1 + A_2 + A_1A_2 + A_1^{-1}A_2 + A_1A_2^2 + A_1^2A_2)). \tag{4.38}$$

Z_{pert} is of the same value as (4.27) in the last section. Note that every Q_{B_i} is proportional to $\mathfrak{q}$, thus the order k is exactly $\sum_{-1}^{2}|\lambda_i|$, which is the total number of boxes for the four Young diagrams λ_i. Partition k to construct the lists of four Young diagrams and sum over all possible Young diagram 4-lists in Z_{G_2}, then we obtain the k-instanton partition function by Mathematica. The results for $k = 2, 3, \ldots$ are a bit tedious, so here we only display the 1-instanton partition function for G_2.

For k=1, the results is

$$Z_{inst}(1) = \frac{2qA_1^3A_2^3(1 + A_1 + A_1A_2)(1 + A_2 + A_1A_2)}{(-1+q)^2(A_1 - A_2)^2(-1 + A_1^2A_2)^2(-1 + A_1A_2^2)^2} \tag{4.39}$$

第 5 章　Conclusion

The 5-brane web diagrams can serve as a powerful platform to provide a deep insight into the dualities between various theories. In this article, we give two ways of constructing 5-brane web diagrams for pure G_2 and take a sip of the S-duality between the 5-brane web diagrams of G_2 and $SU(3)$ with Chern-Simons level $\kappa = 7$. Moreover, we reproduce the 5d Nekrasov partition functions for the two kinds of 5-brane web diagrams for G_2. The expressions of partition functions from two different constructions are non-trivially identical, which are the sum over three and four Young diagrams respectively.

Nevertheless, there are still lots of things requiring further research. For instance, the O-vertex method is proven to be effective in the computation of Nekrasov partition functions of web diagrams with $O5^-$-plane, which extends the topological formalism in some degree. However, the formula for O-vertex on $O5^+$ still needs more considerations, which may help to derive the partition function for $Sp(2N)$ gauge theories. Moreover, we did not consider adding matters to the gauge theories in this article, but more dualities can indeed be discovered if we involve the matters in different representations.

参考文献

[1] GIVEON A, KUTASOV D. Brane Dynamics and Gauge Theory[J/OL]. Rev. Mod. Phys., 1999, 71:983-1084. DOI: 10.1103/RevModPhys.71.983.

[2] HAYASHI H, KIM S S, LEE K, et al. Discrete theta angle from an O5-plane[J/OL]. JHEP, 2017, 11:041. DOI: 10.1007/JHEP11(2017)041.

[3] HAYASHI H, KIM S S, LEE K, et al. 5-brane webs for 5d $\mathcal{N} = 1$ G_2 gauge theories[J/OL]. JHEP, 2018, 03:125. DOI: 10.1007/JHEP03(2018)125.

[4] HAYASHI H, ZHU R D. More on topological vertex formalism for 5-brane webs with O5-plane[J/OL]. JHEP, 2021, 04:292. DOI: 10.1007/JHEP04(2021)292.

[5] HANANY A, WITTEN E. Type IIB superstrings, BPS monopoles, and three-dimensional gauge dynamics[J/OL]. Nucl. Phys. B, 1997, 492:152-190. DOI: 10.1016/S0550-3213(97)00157-0.

[6] JEFFERSON P, KATZ S, KIM H C, et al. On Geometric Classification of 5d SCFTs[J/OL]. JHEP, 2018, 04:103. DOI: 10.1007/JHEP04(2018)103.

[7] BRUNNER I, KARCH A. Branes and six-dimensional fixed points[J/OL]. Phys. Lett. B, 1997, 409:109-116. DOI: 10.1016/S0370-2693(97)00935-0.

[8] AHARONY O, HANANY A. Branes, superpotentials and superconformal fixed points[J/OL]. Nucl. Phys. B, 1997, 504:239-271. DOI: 10.1016/S0550-3213(97)00472-0.

[9] WITTEN E. Bound states of strings and p-branes[J/OL]. Nucl. Phys. B, 1996, 460:335-350. DOI: 10.1016/0550-3213(95)00610-9.

[10] ZAFRIR G. Brane webs and $O5$-planes[J/OL]. JHEP, 2016, 03:109. DOI: 10.1007/JHEP03(2016)109.

[11] INTRILIGATOR K A, MORRISON D R, SEIBERG N. Five-dimensional supersymmetric gauge theories and degenerations of Calabi-Yau spaces[J/OL]. Nucl. Phys. B, 1997, 497:56-100. DOI: 10.1016/S0550-3213(97)00279-4.

[12] NEKRASOV N A. Seiberg-Witten prepotential from instanton counting[J/OL]. Adv. Theor. Math. Phys., 2003, 7(5):831-864. DOI: 10.4310/ATMP.2003.v7.n5.a4.

[13] AGANAGIC M, KLEMM A, MARINO M, et al. The Topological vertex[J/OL]. Commun. Math. Phys., 2005, 254:425-478. DOI: 10.1007/s00220-004-1162-z.

[14] LEUNG N C, VAFA C. Branes and toric geometry[J/OL]. Adv. Theor. Math. Phys., 1998, 2: 91-118. DOI: 10.4310/ATMP.1998.v2.n1.a4.

[15] BENINI F, BENVENUTI S, TACHIKAWA Y. Webs of five-branes and N=2 superconformal field theories[J/OL]. JHEP, 2009, 09:052. DOI: 10.1088/1126-6708/2009/09/052.

[16] KIM S S, YAGI F. Topological vertex formalism with O5-plane[J/OL]. Phys. Rev. D, 2018, 97(2):026011. DOI: 10.1103/PhysRevD.97.026011.

[17] NAWATA S, ZHU R D. Instanton counting and O-vertex[J/OL]. JHEP, 2021, 09:190. DOI: 10.1007/JHEP09(2021)190.

[18] TAKI M. Refined Topological Vertex and Instanton Counting[J/OL]. JHEP, 2008, 03:048. DOI: 10.1088/1126-6708/2008/03/048.

[19] IQBAL A, KASHANI-POOR A K. The Vertex on a strip[J/OL]. Adv. Theor. Math. Phys., 2006, 10(3):317-343. DOI: 10.4310/ATMP.2006.v10.n3.a2.

致　谢

I highly appreciate my supervisor Satoshi Nawata who guided me to this wonderful field and never failed to eliminate my puzzles by patient instructions. Also, I'm deeply indebted to Professor Yidun Wan, who ignited my interest in theoretical physics and led me to the path of being a researcher. Also, I'm very grateful to my friends Zongqi Shen, Zheyuan Zhu, Jiaqi Guo, Chang Shu, Yilu Shao and so on. I learned a lot from them and received great encouragement which supported me to move ahead. Special thanks to Xiangdong Zeng, who is knowledgeable and offered me lots of technical support. Finally, great thanks to my parents for their constant support.

复旦大学
学位论文独创性声明

本人郑重声明：所呈交的学位论文，是本人在导师的指导下，独立进行研究工作所取得的成果。论文中除特别标注的内容外，不包含任何其他个人或机构已经发表或撰写过的研究成果。对本研究做出重要贡献的个人和集体，均已在论文中作了明确的声明并表示了谢意。本声明的法律结果由本人承担。

作者签名：_____ 日期：_____

复旦大学
学位论文使用授权声明

本人完全了解复旦大学有关收藏和利用博士、硕士学位论文的规定，即：学校有权收藏、使用并向国家有关部门或机构送交论文的印刷本和电子版本；允许论文被查阅和借阅；学校可以公布论文的全部或部分内容，可以采用影印、缩印或其它复制手段保存论文。涉密学位论文在解密后遵守此规定。

作者签名：_____ 导师签名：_____ 日期：_____